

This document was produced
by scanning the original publication.

Ce document est le produit d'une
numérisation par balayage
de la publication originale.

OPEN FILE
DOSSIER PUBLIC 718



**PRELIMINARY GEOMATHEMATICAL ANALYSIS OF GEOLOGICAL,
MINERAL OCCURRENCE AND GEOPHYSICAL DATA,
SOUTHERN DISTRICT OF KEEWATIN,
NORTHWEST TERRITORIES**

F.P. Agterberg, C.F. Chung, S.R. Divi,
K.E. Eade and A.G. Fabbri

DEPARTMENT OF ENERGY, MINES AND RESOURCES
GEOLOGICAL SURVEY OF CANADA

MINISTÈRE DE L'ÉNERGIE, DES MINES ET DES RESSOURCES
COMMISSION GÉOLOGIQUE DU CANADA

Ottawa, CANADA

April, 1981
Price: \$5.00

GEOLOGICAL SURVEY OF CANADA

OPEN FILE 718

**PRELIMINARY GEOMATHEMATICAL ANALYSIS OF GEOLOGICAL,
MINERAL OCCURRENCE AND GEOPHYSICAL DATA,
SOUTHERN DISTRICT OF KEEWATIN,
NORTHWEST TERRITORIES**

F.P. Agterberg, C.F. Chung, S.R. Divi, K.E. Eade and A.G. Fabbri

CONTENTS

1	Summary
1	Introduction
2	Classification of rock types and mineral occurrences
3	Quantification of geoscience map data
4	Statistical experiments to relate specific types of mineral occurrences to rock types
5	Volcanogenic massive sulphide deposits (Type 1)
6	Gold occurrences in Archean volcanics (Type 7)
8	Copper mineralization (mainly Cu) in intermediate-mafic volcanic rocks (Type 16)
8	Copper-nickel mineralization in mafic and ultramafic rocks (Type 6)
9	Suggestions for further work
10	References
11	Appendix 1. Statistical experiments on the preferred orientations of Bouguer anomaly contours
	Tables
12	1. Codes for mineral deposit and commodity types
13	2. Rock units coded for the area classified according to lithology and age
14	3. Summary statistics for statistical experiments performed
15	4. Copper-Nickel in mafic and ultramafic rocks
	Figures
in pocket	1. Study area with locations of mineral occurrences
in pocket	2. Simplified geological map of southern part of District of Keewatin used for geomathematical study
16	3. Binary images of square portion of geological map obtained at different resolutions
17	4. Edited binary mosaics
18	5. Line thinning of the binary image of contacts between rock types
18	6. Probability index map for volcanogenic massive sulphide occurrences in cells
19	7. Volcanogenic massive sulphide occurrences. Control area of Fig. 6 was divided into two triangular control areas
20	8. Volcanogenic massive sulphide occurrences. Experiment of Fig. 6 repeated using different control area
20	9. Volcanogenic massive sulphide occurrences. Experiment repeated using study area as control area
21	10. Gold occurrences in Archean volcanic rocks. Diagonal line separates the area into two parts
21	11. Gold occurrences in Archean volcanic rocks. Study area of 1599 cells was used as control area
22	12. Gold occurrences in Archean volcanic rocks. Study area of 644 cells containing Archean volcanic rocks was used as control area
22	13. Gold occurrences in Archean volcanic rocks. Portion of area northwest of diagonal line was used as control area
23	14. Copper mineralization in intermediate-mafic volcanic rocks. Study area of 644 cells containing Archean volcanic rocks was used as control area
23	15. Copper mineralization in intermediate-mafic volcanic rocks. Experiment repeated for smaller control area
24	16. Copper mineralization in intermediate-mafic volcanic rocks. Experiment repeated using 12 instead of 6 variables
24	17. Copper mineralization in intermediate-mafic volcanic rocks. Experiment of Fig. 16 repeated for smaller control area
25	18. Copper-nickel mineralization in mafic and ultramafic rocks. Six deposit cells are shown as circles. Control area is marked by heavy lines
25	19. Copper-nickel mineralization in mafic and ultramafic rocks. Principal components analysis was applied to 143 cells of the control area
26	20. Copper-nickel mineralization in mafic and ultramafic rocks. Experiment repeated using logistic regression
26	21. Bouguer anomaly contours for western part of study area, digitized from gravity maps
27	22. Zebra map for pattern of Fig. 21
28	23. Area of 768 x 768 picture elements covering most of Fig. 22 was subdivided into three subareas
29	24. Histograms showing preferred orientations of gravity contours for subareas shown in Fig. 23
30	25. Histograms showing preferred orientations of gravity contours for nine square subareas
31	26. Simplified rose diagrams derived from histograms shown in Fig. 25

PRELIMINARY GEOMATHEMATICAL ANALYSIS OF GEOLOGICAL, MINERAL OCCURRENCE AND GEOPHYSICAL DATA, SOUTHERN DISTRICT OF KEEWATIN, NORTHWEST TERRITORIES

Summary

The purpose of this study was to conduct a test resource appraisal of the southern part of the District of Keewatin by geomathematical correlation of the locations of known mineral occurrences with regional geological and geophysical data systematically quantified for the entire region. The 174 known mineral occurrences were classified according to deposit and element type (Table 1). Thirty-four generalized rock units were defined and digitized for square picture elements measuring 500 m on a side (Fig. 2).

Multivariate statistical techniques were applied to data for selected occurrences (see Fig. 1) of the following four types: (a) Volcanogenic massive sulphide type; (b) Au in Archean volcanic and sedimentary rocks, gneisses, etc.; (c) Mainly Cu in mafic-intermediate volcanic rocks; and (d) Cu-Ni in mafic and ultramafic rocks. This resulted in a set of probability index maps for each type (see e.g. Fig. 6) with index numbers that indicate the relative favourability of occurrence of mineralization in 10 km x 10 km cells.

For the purposes of illustration and comparison of the probability index maps, it was assumed that there exists a single undiscovered deposit in the region for each of the four types (a-d). When very little geological knowledge is used, the probability that a 10 km x 10 km cell contains this deposit is approximately 0.001 for each type. A probability map with index numbers ranging from 0 to 9 is used to express (1) the strength of association between a deposit type and the geological framework, and (2) the degree to which this association has been captured by the geomathematical model. The probability that the single deposit occurs in a cell belonging to the group of cells with the highest index numbers amounts to (a) 0.023, (b) 0.004, (c) 0.011, and (d) 0.008, for the four types, respectively. These probabilities can be compared with similar probabilities in other regions. For example, the probability that a "favourable" 10 km x 10 km cell in the Abitibi Volcanic Belt of the Superior Province contains a large copper deposit is approximately 0.027.

This report also outlines plans for future work in the southern District of Keewatin using additional information. For the present study, only Bouguer anomaly gravity data were digitized in addition to the regional geology. Incorporation of this geophysical information did not improve the probability index maps for the four deposit types considered. In a special study of the digitized data it was found that the gravity contours show two preferred orientations (northeast-southwest and northwest-southeast) in the entire area. The northeast direction represents the main structural trend in the region and the northwest direction was interpreted as representing a younger trend in the crust associated with granitic plutons that were emplaced after the Hudsonian orogeny.

INTRODUCTION

A proposal to conduct a test resource appraisal in southern District of Keewatin was made in March, 1979. This region was selected because it had already been appraised by preliminary geological analogy methods (Geological Survey of Canada, 1980). Thus the statistical evaluations can be compared with the earlier qualitative appraisals. Another reason for choosing this particular region is to provide a base area on which later more sophisticated "merged" quantitative and qualitative (deposit analogy) appraisals can be constructed.

The study area (see Fig. 1) covers the southern District of Keewatin and a small part of the District of Mackenzie. It consists of NTS Quadrangle 65 and the western part of NTS 55 and is approximately bounded by latitudes 60° and 64° and by Hudson Bay and longitude 104°. A geological compilation of the area, of 1:500 000, by K.E. Eade was used as the geological input for this study. Bouguer anomaly gravity maps (Gibb and Halliday, 1974) also at 1:500 000 scale provided a geophysical input. A total of 174 mineral occurrences in the region have been classified and used in the test resource appraisal.

This report describes results obtained during Phase I of a planned more comprehensive southern Keewatin resource appraisal project. It can be regarded as a pilot study in preparation for a Phase II, during which the geological and mineral deposit data base can be quantified in more detail and considered in conjunction with aeromagnetic and geochemical data.

The present study has several new features. It is a first attempt to apply geomathematical resource evaluation techniques in a frontier region where there has been only one mining operation (North Rankin Ni-Cu deposit) and, overall, less prospecting than in established mining districts in the Canadian Shield. The state of the regional geologic and metallogenic knowledge in the District of Keewatin is much less advanced than in the Abitibi Volcanic Belt and the Canadian Appalachian Region where most previous geomathematical work has taken place. For the first time full use has been made of GIAPP (Geological Image Analysis Program Package) and SIMSAG (System for Interactive graphic computer programs of Multivariate Statistical Analysis of Geological data) systems developed by A.G. Fabbri and C.F. Chung, respectively.

Total time spent on the project was limited to 8 man-months. The work history of Phase I of the project was as follows. The approximately 100 rock units on the geological maps were first grouped into about 34 generalized litho-age units by S.R. Divi and, locally, geological detail on the maps was generalized in preparation for coding. The resultant precoded geological maps and the gravity maps were then digitized in the Computer Graphics Laboratory of National Research Council Canada using GIAPP on the Modcomp II mini computer. A summary of the National Research Council Canada study is given later in this report and further information is in press (Kasvand *et al.*, in press). This work resulted not only in the capability to use GIAPP but also in a number of magnetic tapes for transfer of data from the Modcomp II to the Cyber 74 computer of the Department of Energy, Mines and Resources.

Following the above, computer programming was performed to obtain the cell values (for 10 km x 10 km cells) required as input for SIMSAG which is operational with a 4014 Tektronix graphic terminal on the Cyber 74 computer (see Chung, 1979). Additionally, a number of colour plots of the coded geological map data were obtained using the Applcon plotter of the Geological Survey of Canada. Initial statistical experiments were performed on a preliminary set of 61 copper occurrences.

During the subsequent three months, the mineral deposit data base was extended to 174 occurrences by R.I. Thorpe and R.D. Lancaster who provided new data on other types of mineral occurrences. The new information was added to CANMINDEX (Canadian Mineral Occurrence Index, see Picklyk *et al.*, 1978) by staff of the Mineral

Deposits Data Bank. Computer-generated plots at a scale of 1:500 000 showing the locations of the occurrences were provided by R.M. Laramée. Finally, the 174 mineral occurrences were classified (Table 1) for the purpose of statistical analysis. Only the locations of the 61 mineral occurrences used for the statistical experiments described in this report are shown in Fig. 1.

The preliminary statistical experiments described in this report were conducted during November, 1979. Specific types of mineral occurrences were related to selected rock types by using SIMSAG.

As a special study to extend the use of data, the preferred orientations of the Bouguer anomalies in the southern District of Keewatin were investigated by using the digitized gravity data. Histograms for a number of subareas were constructed by applying the program RODIA (Agterberg, 1979) to covariance data obtained by GIAPP.

The statistical modelling of the mineral occurrences in terms of the geological framework is tentative at present, not only because of the experimental nature of the geomathematical models used so far, but also because there are significant gaps in the geological mapping and mineral exploration data base in the District of Keewatin. Nevertheless, it will be useful to continue with Phase II for the purpose of constructing more sophisticated qualitative and quantitative resource appraisal models based on metallogenic concepts, and performance of special studies to correlate and integrate additional types of geoscience data such as aeromagnetic information.

CLASSIFICATION OF ROCK TYPES AND MINERAL OCCURRENCES

Geological data base

The study area forms the central part of the western portion of the Churchill Province (Fig. 1). Approximately one-half of the area has been mapped at 1:250 000 scale, and a small part at 1:500 000 scale; in the remainder, the base map is from the original reconnaissance mapping at 1:1 000 000 scale. This variability in the scale of map coverage introduces problems in presenting a cohesive interpretation of the geological history of the area. Another problem, as in all of the Churchill Structural Province, is the distinction between the metamorphic effects of the Kenoran Orogeny and those of the younger Hudsonian Orogeny. Geochronological data in this region are limited (Wanless and Eade, 1973); hence, in many places lithological similarities are used as an indication of age equivalence of rocks. The 34 rock units coded for the area are shown in Fig. 2 and Table 2.

Metasedimentary and metavolcanic rocks belonging to the Kaminak Group (Davidson, 1970a, 1970b; Heywood, 1973; LeCheminant et al., 1977) in the north, and the Henik Group (Eade, 1973, 1974) in the south, form part of a belt of Archean rocks that trend northeast from Ennadai Lake to Rankin Inlet (Figs. 1, 2). The volcanic rocks are massive and pillowed basalts (unit 8) and undivided mixed volcanics (unit 7), with minor amounts of intercalated rhyolites, dacites and andesites (unit 6). Areal proportions of mafic, intermediate and felsic volcanic rocks are approximately in the ratio of 10:5:1. Laterally, the volcanic and sedimentary rocks are intercalated, and together with some volcanic arenites, they are represented by unit 5. Tuff and agglomerate are associated with the felsic phases and irregular masses of medium-grained gabbros (unit 10) occur within the mafic flow sequences. Ultramafic rocks (unit 11) occur within mafic lava units in a few localities, but areas of these rocks are commonly too small to show on Fig. 2. The sedimentary rocks consist of conglomerates and arkoses (unit 1) and greywackes and pelites (unit 3). Thin bands of iron formation (unit 4) composed of jasper-hematite, siliceous magnetite-hematite and quartz-magnetite are present mainly

within the greywacke sequence, although west of Montgomery Lake a thin band is associated with mafic lavas (Eade, 1974).

The Archean rocks were deformed, metamorphosed and intruded to varying degrees during the Kenoran orogeny. In general, they are folded about northeasterly plunging axes and metamorphosed from greenschist to granulite facies (Eade, 1978). Some of the mafic volcanic rocks have been in part converted to amphibolite and the sediments metamorphosed to quartzofeldspathic gneisses (unit 12). The rocks commonly grade to granite gneisses through zones of migmatites and mixed gneisses (unit 12). The volcanic and sedimentary rocks, as well as the gneisses, are cut by high-level nearly massive granodiorite, quartz monzonite and syenite (unit 9), and by diorites and gabbros (unit 10).

In large areas in the western part of the region where the only information available is from reconnaissance surveys (Wright, 1967) the ages of granitoid gneisses (unit 15), and mafic (unit 14) and felsic (unit 13) plutonic rocks are unknown. The age of metamorphism is, however, thought to be largely Archean with an overprint of an Aphebian event and probably plutons of both Archean and Aphebian age are present.

The Aphebian rocks are divided into a lower Montgomery Lake Group, a middle Hurwitz Group and an upper Ennadai Group. The Hurwitz Group is widespread and occupies scattered areas along a northeasterly trending belt that approximately coincides with the belt of Archean rocks. The other two groups are restricted in distribution. West of South Henik Lake (Figs. 1, 2), a sequence of conglomerate, arkose and quartzite (unit 16) of the Montgomery Lake Group, unconformably overlies Archean andesites (Eade, 1966). A sequence of conglomerate, orthoquartzite and greywacke of the Padlei and Kinga Formations (unit 18) of the Hurwitz Group unconformably overlies the Montgomery Lake Group. Unit 18 also includes a sequence of similar rocks that are part of the Tavani Formation. Unit 19 represents poorly exposed slate, shale and siltstone of the Ameto Formation. Unit 20 consists of dolomites and argillite of the Watterson and Tavani formations. In many localities the dolomite is overlain by greywacke (unit 21), as for example that of the Ducker Formation. Unit 24, which is very restricted in distribution, represents undivided dacites and andesites of the Watterson Formation. The Hurwitz Group is overlain by the conglomerates and lithic greywackes (unit 26) of the Ennadai Group. The MacKenzie Lake metasediments, which cannot be uniquely correlated with either Archean or Aphebian sedimentary rocks, are included in Unit 15.

The Aphebian rocks were deformed moderately about northeast- and locally northwest-trending fold axes during the Hudsonian orogeny. Contacts between the Hurwitz and Archean rocks are often sheared, indicating movement along contact faults. For the most part, Aphebian rocks are only slightly metamorphosed, although Aphebian intermediate (unit 28) and felsic (unit 27) intrusions produced metamorphic aureoles carrying cordierite and garnet. The paragneiss and migmatite of the Hurwitz Group are denoted by unit 25, and the undivided Aphebian quartzofeldspathic and amphibolitic gneisses are included in unit 29.

Unmetamorphosed continental sedimentary and volcanic rocks of the Dubawnt Group (Paleohelikian) occur from Kamilukuak Lake northeast to the western end of Chesterfield Inlet (Figs. 1, 2) in structurally controlled basins of deposition. At the northeastern end of the belt (south of Baker Lake), a lower redbed sequence (unit 30) of conglomerate, sandstone and siltstone unconformably overlies the Archean metasedimentary and metavolcanic rocks and felsic gneisses (LeCheminant et al., 1977). This sequence consists of the Angikuni and South Channel Formations.

At the southwestern end of the belt only, polymictic conglomerate, sandstone, arkose and siltstone of the Angikuni, South Channel and Kazan Formations or their equivalents overlie the basement rocks. Overlying these sediments are the alkaline Christopher Island volcanic and volcanogenic sedimentary rocks (unit 31). Alkaline intrusions (unit 34) including the Martell syenite belong to this suite. The alkalic suite is overlain by calc-alkalic quartz-feldspar porphyries and associated volcanic rocks (unit 37) of the Pitz Formation. Plutons of granite to quartz monzonite composition form an important part of this calc-alkaline suite. Overlying the Pitz Formation are conglomerate and sandstone (unit 35) of Thelon Formation, basalt (unit 38) and dolostone (unit 36).

Plutons of Nuelin Granite (unit 39) are considered to be of Paleohelikian age, following Stockwell (1972), although Weber *et al.* (1975), working in northern Manitoba, consider them to be late Aphebian. Paleozoic limestone (unit 40) outcrops in a small area northwest of Dubawnt Lake (Figs. 1, 2).

Mineral occurrence data base

Information on 174 mineral occurrences in the area was retrieved from the CANMINDEX file (Picklyk *et al.*, 1978). Although grade and tonnage information, is not ordinarily recorded in this "index level" file, and descriptive geological information is limited, a tentative classification of the 174 occurrences was attempted (Table 1) on the basis of two main criteria – (1) broad geological environment of the occurrence, and (2) elements present in the occurrence. Although this classification is tentative it was a necessary first step for modelling in the statistical analysis. In the models discussed in more detail in later sections of this report, some groupings of occurrences listed in Table 1 are used for control in experiments performed to evaluate the study area for its mineral potential. Control from outside the area has not been considered so far in these statistical experiments, although this will be a useful addition in follow-up work to this preliminary study. It is assumed that the known occurrences in the region are indicative of undiscovered larger mineral deposits of the same types. It is also considered likely that the multivariate expressions derived for the relationship between the proven small mineral deposits and the geological framework also will be valid for the relationship between as yet undiscovered larger mineral deposits and the geological framework. It should also be kept in mind that, while the area under study may hold potential for deposit types not presently represented by known occurrences, these can not be predicted by the present study.

QUANTIFICATION OF GEOLOGICAL AND GEOPHYSICAL MAP DATA

The quantification of the geological maps (scale 1:500 000) and the Bouguer anomaly gravity maps (1:500 000) was performed in the Computer Graphics Laboratory of the Electrical Engineering Division, National Research Council Canada. These quantification procedures are described in more detail elsewhere (Kasvand *et al.*, in press).

The process involved the conversion of the graphic information on the regional geological and geophysical maps to computer-processible format so that the data could be displayed and interpreted as computer-reproducible images. The information on the original maps was in a form which is not suitable for fully-automated processing by means of optical devices. For example, a considerable amount of redrafting would have been required to permit treatment using a flying spot scanner which is an optical device available at National Research Council Canada. The digitization of map information was performed on a graphic tablet. Each 1:500 000 map was subdivided into rectangular subareas of appropriate size and the information in the

subareas was digitized separately. For the most part the map segments used consisted of squares measuring 30½ cm on a side.

An operator using the graphic tablet traces geological contacts or geophysical contours which the computer approximates by sequences of appropriate short line segments (vectors). During this tracing process which is accomplished by means of a pen-like cursor (or stylus) both the trace of the pen and the endpoints of the vectors are displayed on a Tektronix 611 storage display. Some editing can be performed at this stage. The material that is retained is stored on magnetic tape for further usage.

Later, each rectangular subarea is converted to two-dimensional binary form and stored as a matrix or binary picture. This procedure is equivalent to superimposing a sheet of transparent squared paper onto the subarea and marking a square as a one (1) if a contact (contour) line crosses the square, and as a zero (0) if there is no contact in the square. Obviously the resolution of a binary map depends on the size of the squares chosen. These squares are called picture elements or pixels. The centers of the squares are raster points belonging to a grid. The present maximum size for a single binary submap is 512 x 512 picture elements. Most binary submaps used in this study were 305 x 305 picture elements. Fig. 3 shows the results of three experiments performed in order to select an adequate resolution for the precoded 1:500 000 geological maps. The binary map (Fig. 3c) with picture elements measuring 375 m on a side provides the best approximation in that it closely resembles the map image stored in vector mode. On the other hand, the binary map for 1 km resolution (Fig. 3a) is least satisfactory because the shapes of some contacts are distorted and some areas enclosed between separate contacts have disappeared. For our study, an intermediate 500 m resolution was selected. Binary subarea maps can be combined to form binary mosaics with a maximum size of 1024 x 1024 picture elements. The accuracy with which one submap can be aligned with another is in the order of one picture element. Fig. 2 was constructed from the information shown on Fig. 4 which consists of two separate square binary mosaics with 915 x 915 (Fig. 4a) and 610 x 610 (Fig. 4b) picture elements, respectively. Thus the 500 m resolution allows the 1:500 000 maps for the entire study region to be represented on only two binary images. In general, a twofold increase in resolution (e.g. from 500 m to 250 m) enlarges the number of binary images by a factor of four. Subsequent computing time also increases significantly when the resolution is improved. This is the main reason for attempting to keep the total number of binary images as small as possible.

The binary images shown in Fig. 4 have been edited as can be seen by comparing Fig. 3b to its corresponding area in the southwestern corner of Fig. 4b. Due to the resolution of the binary maps, some very small areas may become closed, some adjacent contacts may touch and break or other defects may occur. To ascertain that the pattern of the binary map corresponds as well as possible to that of the original, the binary map is printed and checked. Whenever feasible, the defects are removed by adding or deleting contact pixels. The amount of editing required is larger when the resolution is poorer.

As a final step the thickness of the contact contour lines is automatically reduced to a minimum while preserving connectivity of lines by a process called line thinning which is illustrated in Fig. 5. The application of the preceding operations resulted in the pictures shown in Fig. 4.

For identification, a unique label or serial number is automatically assigned to each area in the picture that is enclosed by the lines. At this stage the picture is no longer binary. It is a component labelled image. The number of phases or map units (e.g. litho-age units) is less than the total

number of enclosed areas because generally a map unit has more than a single exposure area. The online operator assigns a unique serial number to each phase by employing a semi-automatic process carried out via interactive displays. The computer matches the map unit labels with the enclosed area labels. If it is felt at this stage that additional modifications should be made in the digital image, it will be necessary to return to earlier stages in the process of digitization.

The image can be used in different ways. Binary images of rock types or combinations of rock types can be created for further study. In our study, each digital image was stored on magnetic tape for transfer to the Cyber Computer System at the Department of Energy, Mines and Resources.

The preceding procedure was also applied to the gravity maps. Two digital images corresponding to those for the geological maps were prepared showing Bouguer anomaly contours at 5 milligal intervals. The labels (serial numbers) 7-23 were assigned to successive intervals between -10 and -95 milligals, the total range of the Bouguer anomaly values in the study area. For example, a label value of 15 was used for raster points with a Bouguer anomaly between -50 and -55 milligals.

Two corresponding digital images have been prepared for the 174 mineral occurrences labelled according to the classification discussed in the previous section. Each mineral occurrence was assigned to the 500 m x 500 m picture element in which it occurs. This introduces an error in location of the occurrences of up to 250 metres in both the east-west and north-south direction.

In total, therefore, six magnetic tapes were prepared, one for each digital image. The geology, gravity data and mineral occurrences each were represented on two tapes with information for the same pairs of arrays of 915 x 915 and of 610 x 610 picture elements, respectively. These pixels correspond to squares measuring 1 x 1 mm on the 1:500 000 map or 500 x 500 m on actual ground surface. For the geological and geophysical data, the picture elements representing contacts were labelled separately.

On the Cyber 74 network of the Department of Energy, Mines and Resources the information for blocks of 20 x 20 picture elements was combined yielding input data for SIMSAG with information on 10 x 10 km cells. In shape and size, these cells correspond to the cells previously used for multivariate statistical analysis in the Abitibi area (Agterberg et al., 1972) and Appalachian Region (Leech, 1975). In these earlier studies, the 10 x 10 km cells for geological and geophysical data were point-counted by subdividing them into 400 subcells measuring 500 m on a side and coding the presence or absence of a rock type or phase at the midpoint of each subcell.

The numerical cell data for the southern Keewatin area range from 0 to 400 for every rock type in every cell. The maximum (=400) would be reached if a 10 x 10 km cell is fully occupied by a given rock type. The amount of contact as represented by the number of picture elements on the boundaries between rock types in the digital images was determined separately as a new variable.

STATISTICAL EXPERIMENTS TO RELATE SPECIFIC TYPES OF MINERAL OCCURRENCES TO ROCK TYPES USING SIMSAG

The system SIMSAG has recently been described by Chung (1979). Its capabilities can be briefly summarized as follows. SIMSAG enables the user to manipulate variables, select areas, and perform multivariate statistical analysis. All operations and commands in the system are interactively performed and the data or results are graphically displayed

on the user's terminal. The system is in Fortran and operational with a 4014/5 series Tektronix graphic terminal on the CDC Cyber 74 computer network.

Typically, the system works with several thousands of cells with values for the variables quantified for the geological framework of a region. Each cell is characterized by its x and y coordinates for geographic location and by the values of the variables.

Subareas containing fewer cells than the entire data base can be selected by specifying the x and y coordinates of the cells to be included. Alternatively, a criterion set can be specified, such as, for example, having cells from within a rectangular area bounded by lines with given values of x and y and which contain at least one of several given rock types forming the subarea. It is also possible to select a subarea by drawing a polygon on the screen. Then cells with centers inside the polygon are selected (or deleted).

The variables can be modified according to one or more of the following capacities:

- (1) Selection or deletion of variables;
- (2) Deletion of variables whose observed values for all cells are equal to a constant (e.g. zero);
- (3) Definition of new variables that are functions of the existing variables;
- (4) Transformation of variables into any functional form; including the binary (0-1) form which indicates presence or absence of a rock type in a cell.

SIMSAG contains at present eight multivariate statistical techniques: (1) principal components analysis; (2) discriminant analysis; (3) multiple regression analysis; (4) stepwise regression analysis; (5) logistic regression analysis; (6) Poisson regression analysis; (7) characteristic analysis; and (8) the user can assign a weighting factor to each variable. These weighting factors need not have been determined by means of one of the preceding methods, e.g. subjective weighting factors can be used.

A typical run with SIMSAG applied to cell values for a region proceeds as follows. First a set of "deposit cells" is defined, each of which contains one or more mineral deposits or occurrences of a specific type. Next a control area is defined which constitutes only part of the complete area studied. The variables are subjected to suitable transformations. Then, in the control area, weighting factors are computed for all transformed variables by choosing one of the preceding methods of multivariate statistical analysis. The sum of the weighted variables is displayed for the control area and also for the entire area of study.

In this study, stepwise regression analysis, one of the multivariate statistical techniques available in SIMSAG, was the primary method used for estimating the mineral potential. In a case such as this, use of any regression model is based on the assumption that the probability of presence of a mineral occurrence is a function of the geological attributes that have been mapped in a region. The application of regression analysis for estimating the correlations must be preceded by the selection of areas and geological variables to be used for the analysis. To avoid confusion, several terms have been defined as follows for this type of work. A cell is called a "deposit cell" for a given type of mineralization if it contains one or more known occurrences of that type. The "study area" for a given type of mineralization consists of all the cells which contain at least one picture element of "related" geological variables for that type. For example, cells without any Archean rocks would not be contained in the study area for a group of Archean mineral occurrences. The "control area" is the part of the study area where regression analysis is applied for estimating the correlations. The "target area" is the part of the study area which is outside the control area.

Selection of the control area in the study area may be a rather arbitrary process. In particular, one of the implications of the concept of a control area is that all mineral occurrences of a given type are known within the control area. Obviously, the control area must contain at least one of the deposit cells because, otherwise, no relationships between geological variables and mineral occurrences can be evaluated. On the other hand, when the control area contains all known occurrences of that type within the region under study, it may be difficult to evaluate the results of the analysis because then there are no known deposits in the target area for verification.

As noted, the selection of geological variables presents another difficulty in application of regression analysis. The simplest method, often yielding meaningful results, is consideration of all geological variables that occur in the deposit cells regardless of whether or not they are held to be genetically related to the deposits. The relationship of each geological variable with the known occurrences then can be evaluated independently and statistically tested. Variables that are statistically significant at a specified level of significance are then selected for the regression analysis.

However, the preceding selection procedure may generate results which are not necessarily geologically meaningful. For instance, using the above procedure, the gold occurrences in Archean volcanics (type 7 of Table 1) turn out to be significantly spatially correlated with the Aphebian-Hurwitz carbonate (unit 20 or g20) and thus g20 would be selected for the regression model for the gold occurrences. However, only a few of the gold deposits occur in Archean mafic volcanics that are in contact with g20, and the occurrence of g20 itself is restricted only to a few cells. In this case, the conditions for selection seem to be artificial and local characteristics of this type should not be used for resource analysis. On the other hand, it is possible that some of the gold occurrences in Archean rocks have ages younger than Archean. In that case, the correlation with g20 may, in fact, be meaningful.

Hence, geological variables that were believed to be unrelated genetically with the occurrences were not considered in the regression analysis. However, it is also meaningless to select all geological variables which could be genetically related with the deposits when the correlation is not statistically significant. For this reason, the stepwise regression method has been extensively used for selections of the variables. The complete method (cf. Agterberg *et al.*, 1972) consists essentially of the following five steps:

1. Consider all geological variables that (a) occur in the deposit cells and (b) are believed possibly to be genetically related to the deposits.
2. Taking each variable separately, correlate the geological variables with the known occurrences in the control area. Select the variable with the highest correlation.
3. Taking each variable separately, correlate those variables which have not yet been selected with the unexplained known occurrences. Select the variable with the highest correlation if the correlation is statistically significant.
4. Except for the variable last selected (in step 3), test the variables selected previously by correlation with the unexplained portion of the occurrences. If one or more of the variables selected previously are superseded by new variables, delete the earlier variables (step 3).

5. Repeat steps 3 and 4 until all the variables have been considered. In the significance tests carried out during these steps, a variable is selected (or deleted) only if it meets (or fails) the "significance level for selection" set equal to a constant value (e.g. = 0.4) for every experiment (cf. Agterberg *et al.*, 1972).

After selecting several variables using the stepwise regression technique, logistic regression analysis and ordinary regression analysis, were applied in most experiments. However, the results of these two techniques usually were not greatly different and are not shown separately in this report.

Four types of occurrences were separately analyzed with the results to be described in the next sections. Table 3 contains summary statistics for all statistical experiments to be described. Each experiment resulted in a set of values (probability index map, cf. Agterberg *et al.*, 1972) calculated for all cells in the study area. For convenience, these values were rescaled so that for each probability index map they range from 0,1,..., to 10(=A). The actual minimum value and maximum value (=A) obtained in the control area are given in Table 3 for each run. The maximum value (A) is shown on the Taktrox screen as A for reference purposes. All other values are ranked in relative importance from zero to 9 using ten classes with equidistant class limits along the interval between minimum and maximum value of the control area.

VOLCANOGENIC MASSIVE SULPHIDE MINERALIZATION (TYPE 1)

The twelve known mineral occurrences of this type are regionally associated with a belt of Archean metavolcanic-metasedimentary and plutonic rocks that trends northeast from Ennadai Lake to Rankin Inlet (Fig. 2). The geological variables g3, g6, g7, g8, g9, g10 and g18 in various proportions occur in 11 deposit cells. However, variable g18 representing conglomerate, arkose and quartzite of the Aphebian Hurwitz Group was not considered for statistical analysis, because it is assumed to be metallogenetically unrelated to this type of mineralization.

Initially, gravity was used in the statistical analysis along with the six geological variables, but it was eliminated as a variable during the stepwise regression in all experiments. The scale of the gravity data (broadest type of reconnaissance) is such that it would be virtually impossible to relate it directly to the mineralization types. It is in fact difficult in many cases to relate it to lithological types except when these are areally extensive. Hence it is not surprising that the cell values for gravity (ranging from 7 to 23, see before) are uncorrelated with the known mineral occurrences. It is possible, nevertheless, that resolution of the gravity data into "trends" and "residuals" or using them to qualify the lithological data will lead to useful results. For example, felsic volcanic rocks in cells with a higher than average Bouguer anomaly may be underlain by a relatively thick pile of mafic volcanic rocks and this could be relevant to mineralization. Special studies of this type have not yet been undertaken.

Results of five statistical experiments on a study area of 644 cells, each containing at least one of the three Archean volcanic rock units g6, g7 or g8 are shown in Figs. 6-9. The criteria used for selecting this study area of 644 cells are discussed in more detail at the beginning of the next section (No. 6) dealing with gold occurrences in Archean rocks. Each of the five experiments utilized a different control area, in order to investigate the stability of results for the study area. In Fig. 6 the rectangular area outlined, containing all 11 deposit cells, is the control area. The control areas in Figs. 7a, 7b and 8 are smaller, each including only some of the 11 deposit cells. For Fig. 9, the entire study area was considered as the control area. The results in

Figs. 6-9 were obtained by means of stepwise regression analysis, although other statistical methods such as logistic regression analysis were applied for comparison or corroboration. The binary (0-1) form indicating presence or absence of a rock type in a cell was employed for all variables.

Initially, stepwise regression analysis of the control area in Fig. 9 resulted in the selection of variables g7 and g10 at a high level of significance. Other variables entered the regression later. Selection of the intermediate-mafic intrusive rocks (variable g10) at a high level of significance was taken to imply, perhaps, that a geological environment containing both volcanic rocks (mixed) and intrusive rocks (synvolcanic heat source?) may be more favourable for mineralization of this type than an environment with volcanic rocks alone. To investigate this possibility, six new variables representing the coexisting occurrence of different types of Archean volcanic and intrusive rocks were defined, and regression analysis was repeated using all 12 (i.e. 6+6) variables. The new variable defining the joint occurrence of mixed volcanic and intermediate-mafic intrusive rocks (g7 x g10) was selected first in the regression, followed by g6 x g10 for coexistence of felsic volcanic rocks and intermediate-mafic intrusive rocks. For the five control areas in Figs. 6-9, in general, variables g7 and g10 were first selected in the regression when the six variables were used as input variables. However, when the six joint occurrence variables were also included among the input variables for the analysis, the combined variable g7 x g10 was selected first for the control areas in Figs. 7a, 8 and 9; for the control areas in Figs. 6 and 7b, variables g7 and g10 were selected first.

Using the regression coefficient of the variables selected at the 60 per cent significance level, five probability index maps were constructed (Figs. 6-9) for the study area. The values in the study area were scaled to become values ranging from 0 to 10 (= A in Figs. 6-9). The four patterns in Figs. 6, 7a, 8 and 9 are essentially similar, although they differ locally in minor detail. The pattern of values in Fig. 7b, however, is considerably different from and contains more higher values (>8) than those for the other four control areas. In general, the deposit cells have high values, indicating a moderately good fit. A significant observation in Figs. 6, 7a, 8 and 9 is that, in addition to the high values for several of the deposit cells, there are 5 to 8 cells with highest values (>8). These cells have essentially the same location in all four diagrams (Figs. 6, 8a, 8 and 9), i.e. near Carr Lake-Maguse Lake, Heninga Lake to the southwest and Quartzite Lake-Munro Lake to the northeast. It is interesting to note that earlier workers (Ridler, 1971; Ridler and Shilts, 1974) speculated on the presence of volcanic centers in these general areas. Additionally, as noted earlier, the present study brings out the importance of intermediate-mafic intrusive bodies (g10) associated with volcanic rocks for mineralization of this type. At present, variable g10 contains a variety of rock types. It will be interesting to disaggregate it as much as possible in the statistical experiments planned for Phase II of this project.

Assuming that the metallogenetic and statistical modelling of the relationships between mineral occurrences and associated lithologies for the study area are valid, the results can be evaluated in the following simple manner. Suppose that there exists a single cell with undiscovered mineralization in the study area. Without any kind of modelling, the probability (p_1) that a particular cell among the 633 (i.e. 644-11) cells containing Archean volcanic rocks is the cell with mineralization is equal to $1/633 = 0.16\%$. The results in Fig. 6 indicate that there are 20 cells with relatively high values (>7). Four of the 11 known deposit cells are known to occur in the 20 cells. Consequently, the probability (p_2) that a particular cell among the 16 cells without deposits is the mineralized cell is given by $p_2 = (1/16) \times (4/11) = 2.27\%$. The probability of identifying

the mineralized cell therefore has increased by a factor of approximately 14 (i.e. p_2/p_1). The preceding expression for p_2 can be regarded as the product of two probabilities; (a) $1/16$ representing the unconditional probability that the mineralized cell is one of the $(20-4)=16$ cells with a probability index of 7 or more and without known occurrences, and (b) $4/11$ representing the probability that a cell with known occurrences also has a higher than average value. The resulting probability p_2 is a simple and convenient measure of the favourability of a particular geological environment for undiscovered deposits of the type being studied.

None of the volcanogenic massive sulphide deposits considered is known to be large. In the preceding simple analysis, the probability that a deposit occurs in a cell with known mineralization was set equal to zero. On the contrary, it seems reasonable to assume that the probability of a large deposit occurring in a cell with known mineralization is higher than average and should not be set equal to zero. For this reason, the following, slightly different statistical model has also been applied.

Suppose that the geological environment of the known occurrences of volcanogenic massive sulphide deposits is representative of the occurrence of an undiscovered large deposit of the same type. In order to formalize this assumption, it is useful to define two binary random variables (1) X for occurrence of a favourable geological environment, and (2) Y for occurrence of the large deposit. Each of these binary variables is either 1.0 or 0.0 for a specific cell. X assumes the value 1.0 when the probability index is greater than a specific value (>7 in the example of Fig. 6). These definitions permit the estimation of the conditional probability $P(Y=1 | X=1)$ that the large deposit occurs in a cell with value of 7 or more, from the following four probabilities that are known: (1) $P(Y=1)=a=1/644$ being the unconditional probability that any one of the 644 cells contains the large deposit; (2) $P(X=1 | Y=1)=b=4/11$ representing the probability of a value of 7 or more in the cell containing the large deposit. (This probability follows from the assumption that the environment of the known occurrences is representative of that of the undiscovered large deposit); (3) $P(Y=0)=c=43/644$ being the unconditional probability that a cell does not contain the large deposit; and (4) $P(X=1 | Y=0)=d=16/633$ representing the probability of a value of 7 or more in a cell not containing the large deposit. According to Bayes' theorem, $P(Y=1 | X=1)=ab/(ab+cd)=0.0219$. This result is close to $p_2=0.0227$ obtained earlier by the simpler method.

It is possible to test the correlation between the preceding random variables X and Y for its statistical significance. The conventional chi-squared test for (2x2) contingency tables (with Yates' continuity correction) gives $X(1)=30.66$ which is much greater than $\chi^2_{0.05}=3.84$ for a single degree of freedom and level of significance $\alpha=0.05$. This shows that the correlation between X and Y is statistically significant.

GOLD OCCURRENCES IN ARCHEAN VOLCANICS (TYPE 7)

The 23 occurrences of this type are distributed in 17 cells numbered 1 to 17 in Fig. 10. The 17 deposit cells contain 12 geological variables, g3, g6, g7, g8, g9, g10, g12 (Archean), g15 (Archean/Aphebian), g18, g19, g20, g21 (Apebian-Hurwitz). Fourteen of the 17 cells contain Archean mafic volcanic rocks (g8). Cell 11 contains Archean mixed volcanic rocks (g7). However, the other two cells, Nos. 2 and 7 in Fig. 10, do not contain any Archean volcanic rocks. The occurrence in cell 7 is located at the contact between two Apebian (Hurwitz) rock units (g18 and g20) and occurs outside of the belt of Archean rocks. It could be that this occurrence is misclassified. The occurrence of cell 2 is

at the contact between two Archean rock types (g10 and g12) which are not volcanic. It remains possible that this occurrence is associated with Archean volcanics in a belt that is too narrow to be shown on the digitized map. These two deposit cells (2 and 7) have not been used for the statistical analysis.

The four Aphebian-Hurwitz rocks (g18, g19, g20, g21) have not been considered in the statistical analysis, because the gold occurrences of Type 7 were assumed to be unrelated genetically to geological units with ages other than Archean. The Archean/Aphebian gneiss (g15) was also eliminated from the analysis, because it occurs in only one deposit cell (1). In addition, the three Archean volcanic rock units (g6, g7 and g8) are considered in combination as a single variable because, as noted above, the mixed volcanic rocks (g7) occur in only one cell and felsic volcanic rocks (g6) occur in only two cells. This newly defined variable (g6+g7+g8) occurs in 644 cells in the region.

Subsequently, the Archean volcanic rocks AV=(g6+g7+g8), graywacke (g3), gneiss (g12) and two igneous plutonic rock units (g9 and g10) were transformed into binary variables by replacing the numerical value for all five variables by 1 for cells where the variable is present and maintaining the zero when the variable is absent.

In addition, ten variables for cross products of pairs of the five binary variables were considered. These ten newly defined variables are g3xAV, g3xg9, g3xg10, g3xg12, AVxg9, AVxg10, AVxg12, g9xg12, g9xg10, g9xg12 and g10xg12, where AV is the Archean volcanic variable (g6+g7+g8).

As a study area, first, all the cells which contain any one of the five binary variables (at least one of the five variables assumes value 1) are considered. Later, a small study area which consists of the cells with only Archean volcanics will also be used.

The first experiment is based on the study area that consists of 1599 cells containing one or more of the five binary geological variables. Using stepwise regression analysis, five variables among the fifteen input variables have been selected for the regression model at a significance level of 0.1. The first variable entered into the model was Archean volcanics (AV=g6+g7+g8), which is most significantly correlated with the gold occurrences. After AV the next four significantly correlated variables are g9xg10, g3xg9, g3xg10 and g3xAV.

A probability index map (Fig. 11) for the occurrences of this type has been constructed using the preceding five variables. The 64 cells with values of 8, 9 or A, which have the highest potential for occurrences of type 7, include four known deposit cells. The 198 cells with values of 6 or 7 include eight known deposit cells.

A simple interpretation of this probability index map is as follows. Suppose that there is an unknown deposit cell in the region besides the fifteen known deposit cells. The probability p_1 that any particular cell in the study area is the unknown deposit cell, is $p_1 = (1599-15)^{-1} = 0.06\%$ which is very low, but it can be easily increased by using additional geological information. For instance, the presence of Archean volcanic rocks (AV) is an essential geological characteristic for this type of occurrence so that it may be assumed that the unknown occurrence should be located in a cell with Archean volcanics. There are 644 cells containing Archean volcanic rocks in the study area and all fifteen known deposit cells are included in these 644 cells. From this assumption, it follows that the probability p_2 that any particular cell among the 644 cells is the unknown deposit cell, is $p_2 = (644-15)^{-1} = 0.16\%$ which is nearly 2.5 times larger than p_1 .

The odds can be improved further using the probability index map. The probability p_3 that one of the 198 cells with a value of 6 or 7 in Fig. 11 is the deposit cell $p_3 = (198-8)^{-1}(8/15) = 0.28\%$ because 8 of the known deposit cells are included in these 198 cells. Furthermore, the probability p_4 that any particular cell of the 64 highest value cells is the unknown deposit cell $p_4 = (64-4)^{-1}(4/15) = 0.44\%$.

Consequently, the probability of finding the unknown deposit cell among the 64 cells is 2.8 times higher than that of finding it among the 644 cells containing Archean volcanic rocks.

For the second experiment, stepwise regression analysis was again applied to the ten variables, consisting of four types of Archean rocks (g3, g10, g9, g12) and their six cross products. Six variables (g3, g10, g10xg12, g3xg9, g3xg10, g9xg10) were selected for this model. The significance level for selection was lowered to 0.5 for this run.

The probability index map constructed for this experiment (Fig. 12) is almost identical to the one of Fig. 11. This may imply that in addition to Archean volcanic rocks the potential for the presence of gold occurrences also is controlled by other factors including the presence of graywacke (g3) and igneous plutonic rocks (g9 and g10).

Statistical tests such as analysis of variance have been performed as part of the application of the regression techniques, but direct interpretations of these tests cannot be made because some basic conditions required for applicability of the tests (e.g. independence and normality of the residuals) are not fulfilled. However, empirical tests can be easily performed to compare the probability index maps with the known occurrences. For an empirical test of this type, the study area of 644 cells was divided into two parts as shown in Fig. 10. The northwestern part consists of 375 cells and includes seven deposit cells. The southeastern part contains the remaining 269 cells which include eight deposit cells.

Suppose that the southeastern part is an unexplored area and no deposit cell is known in it. Using the six variables selected for the previous experiment (Fig. 12), logistic regression analysis was applied to cells in the northwestern part only and statistical correlations were estimated. From the relationships for the northwestern part, the mineral potential of the cells in the southeastern part could be estimated. These results are shown in Fig. 13.

In Fig. 13, there are 22 cells with values of 6 or A and which thus have the highest potential in the southeastern part, followed by the 73 cells with a value of 3. Suppose that there are eight unknown deposit cells in the southeastern part (in fact, there are eight deposit cells in this part but these have not been used for analysis). Then the probability \hat{p} that a given cell among the 22 cells is one of the eight deposit cells can be estimated from the probability index map in Fig. 13 as $\hat{p} = 8 \times (2/7) \times (1/22) = 10.39\%$ because, in the northwestern part, two of the seven deposit cells belong to the group of 22 cells with highest values (6 or A). However, since we already know the location of the eight deposit cells, two of which occur in the 22 highest value cells, we can calculate the true value of p as $p = 2/22 = 9.09\%$. The value of \hat{p} is not very different from that of p . Without the probability index map, all we could do is take a cell at random from among the 269 cells, because they are equally likely to contain a deposit. Then the probability that the selected cell is one of the deposit cells is only $8/269 = 2.97\%$. By choosing from among the 22 cells, the probability of finding deposit cells, therefore, is increased 3.5 times.

In the preceding experiment (Fig. 13), the southeastern part was assumed to be the unexplored area. Of course, we also can assume that the northwestern part in Fig. 13 is the

unexplored area and derive the probability index map on the basis of the known occurrences in the southeastern part. For the 32 highest values in the northwestern part, β then amounts to 7.14%, whereas $p = 6.25\%$.

It can be concluded that the patterns of Figs. 11, 12 and 13 are quite similar to each other. This implies that the statistical relationships which have been derived from the data are stable. This stability property is important, in particular when the estimation of unknown resources is to be attempted.

COPPER MINERALIZATION (MAINLY Cu) IN INTERMEDIATE-MAFIC VOLCANIC ROCKS (TYPE 16)

The sixteen mineral occurrences of this type are contained in 12 deposit cells. They are closely associated with Archean rocks, although some Aphebian rocks are also present in the vicinity of a few occurrences. The 12 deposit cells contain geological variables g3, g6, g7, g8, g9, g10, g12, g18, g20 and g29. However, Archean and Aphebian quartzofeldspathic gneisses (g12 and g29), and sandstones and carbonates (g18 and g20) belonging to the Hurwitz Group were assumed to be metallogenetically unrelated to this type of mineralization, and therefore were not used in the statistical analysis. The 644 cells containing Archean volcanic rocks formed the study area for statistical analysis. Together with the six variables, gravity was initially used as an input variable. However, as in the case of the volcanogenic massive sulphide mineralization (Type 1, Section 5) it was not selected during any of the stepwise regressions applied. Two control areas were used in order to compare the results and evaluate the stability of the patterns. For the experiments shown in Figs. 14 and 16, the entire study area was the control area, whereas for the experiments shown in Figs. 15 and 17 a smaller control area, outlined on the figures, was used.

Regression analysis employing control areas of both sizes (Figs. 14, 15) defined variable g8 (Archean mafic volcanic rocks) as the most important rock unit relating to mineralization of this type. Variable g10 (intermediate-mafic intrusive rocks) was selected next for the regression results shown in Fig. 14. In addition, variable g9 (felsic intrusive rocks) was defined as important for the smaller control area shown in Fig. 15. If some of the 16 mineral occurrences actually belong to Type 1 (i.e. volcanogenic massive sulphide deposits), an association of intrusive bodies with the volcanic rocks would, according to the results we presented earlier in this report, be preferable for mineralization. To incorporate such a possibility into the input variables for the analysis, 6 new variables representing cross-products of 3 volcanic and 2 intrusive units were defined.

Regression analysis was performed again for the two control areas, this time using the 12 variables (i.e. 6 + 6). For the larger control area in Fig. 16 the analysis again resulted in variable g8 (mafic volcanic rocks) being selected first and the new variable representing the cross-product $g7 \times g10$ later. However, for the smaller control area, the cross-product of intermediate-mafic volcanic rocks and intermediate mafic intrusive bodies was selected first, and mafic volcanic rocks alone later.

Using the variables selected at a 0.4 level of significance, four probability index maps (Figs. 14-17) were constructed. Although the regional patterns of values in Figures 14 and 15 are similar, there are nearly twice as many cells with a value of 9 or higher when the control area is smaller (Fig. 15) than when it is larger (Fig. 14). This is because, as pointed out earlier, felsic intrusive rocks (variable 9) also attained importance for the smaller control area. This is the reason, for example, that there are high values (Fig. 15) at the northern end of Kaminuriak Lake

where the mafic volcanic belt is closely associated with felsic intrusive rocks. However, the patterns obtained when the 12 (instead of 6 as before) variables are used are more similar for the two control areas (Figs. 16, 17). The improvement in stability of the results could imply that consideration of the factor representing the joint occurrence of volcanic and intrusive rocks is appropriate, perhaps, as noted, because some of the mineral occurrences classified as of this type actually belong to Type 1.

As before, the results may be evaluated in the following manner. If we suppose that there exists an undiscovered mineralized cell in the study area of 632 (=644-12) cells with Archean volcanics, then the probability (p_1) of discovering that cell without the statistical modelling in this study is equivalent to $1/(644-12) = 0.16\%$. On the other hand, there are 60 cells in Fig. 14 with values greater than six, which is approximately the average value of the deposit cells, and these cells thus have a relatively high potential for mineralization. The probability (p_2) that one of these cells is the mineralized cell is equal to $(1/57) \times (3/12) = 0.44\%$, which is nearly 3 times p_1 . A similar result can be obtained for cells with values greater than 7 in Fig. 15. On considering the 12 variables, the number of cells indicating high potential for mineralization is approximately 25 (Figs. 16, 17). Therefore, the probability (p_3) of identifying the mineralized cell is $(1/22) \times (3/12) = 1.14\%$. Consequently, the probability of identifying the mineralized cell has been increased by a factor of 7 after using metallogenic and statistical modelling.

COPPER-NICKEL MINERALIZATION IN MAFIC AND ULTRAMAFIC ROCKS (TYPE 6)

The experiments which follow represent an attempt to model Cu-Ni mineralization, and were undertaken because this type of mineralization forms a good example of a case in which little information is available.

Ten Cu-Ni occurrences in mafic and ultramafic rocks are known in the area studied but little information beyond their location is available on them. They are within or are closely associated with Archean mafic volcanic rocks and mafic intrusions. Ultramafic intrusions are mentioned as part of the host rocks for two of the ten occurrences but these rocks are not shown on any of the maps presently available, the Archean ultramafic rocks having been combined in map units with mafic intrusives. The distribution of the Cu-Ni "deposit cells" is shown in Fig. 18 by the symbol (o). Cell occupancy, the geological composition of the deposit cells, the host rocks for the mineralization (with the exception of ultramafic intrusions), and some related statistics are listed in Table 4. This table summarizes the information available for building models for the identification of cells in the data base which closely resemble the deposit cells. The geological map units which host the occurrences, according to the limited data presently available, are underlined in Table 4. For each unit, the total number of cells in which it is present is given. We can see, for example, that unit g8 (Archean mafic volcanic rocks) occurs in all six deposit cells, and in 560 cells in total. Four deposit cells contain g10 (Archean intermediate-mafic igneous rocks), which occurs in 245 cells. Two deposit cells contain Archean felsic volcanic rocks (g6), and these are present in 61 cells.

In order to quickly gain some insight into the content of the data base in Table 4, two selective retrievals were obtained as follows. In Fig. 18 cells in which g8 occurs together with g10 (Archean mafic volcanic rocks together with intermediate-mafic igneous rocks) are identified by the symbol (/). There are 169 such cells and we can easily locate the deposit cells (o) among them. A more strict condition can be imposed by retrieving all cells with the association $g7-g8-g10-g12$, found in cell 2 of Table 4. This pattern of

cells is identified by the symbol (\) in Fig. 18. There are only 4 cells of this kind in the study area, of which only one is a deposit cell. These two patterns of cell distributions display graphically the association information contained in the data base. In modelling for a prediction experiment we do not want to be too strict in retrieval conditions, in order to avoid merely retrieving the pattern of the deposit cells as a result, nor do we want to be too general in the retrieval and thereby getting a pattern of cells very close to the initial distribution for the geological map units. Therefore we have to ask what associations we can choose, in terms of the map units in the deposit cells, that will define environmental characteristics for Cu-Ni occurrences and can be used to weigh or classify all other cells without known occurrences into those likely to and those unlikely to contain occurrences.

A tentative control area was selected that consisted of the set of all 10 km by 10 km cells contained within six 50 km by 50 km cells centered on the deposit cells. The distribution pattern of these cells is shown in Fig. 18 by heavy outlines. There are 143 cells and geological data are available for them. The study area for the experiments which follow consists of all cells that contain at least one of the geological map units present in the six deposit cells. There are 1599 cells in this study area.

The techniques of principal component analysis and logistic regression analysis were applied to the control and study areas described.

A first experiment applied to the 143 cells of the control area, uses as variables the values for the map units g6, g7, g8, g10 and g12. The first principal component obtained (with coefficients 0.465, 0.065, 0.590, 0.131, and -0.644, respectively for the 5 variables used) explains 25% of the total variation. It is mainly controlled by variables g6, g8 and g12. In particular, the presence of g6 and g8 (Archean volcanic rocks) and the absence of g12 (Archean gneisses) yield the highest scores of the first component. The first component explains deposit cells 3, 4, 5, and 6, but not deposit cells 1 and 2.

The scores for the first component were computed for all the cells in the study area (see Fig. 19). Four deposit cells (o) are included in the derived pattern of high score cells (/ highest and \ next highest scores). There are 84 of these cells in Fig. 19. The first component assumes a high value in many of the 143 cells of the control area which, therefore, represents a broad environment for the deposit cells of Type 6.

Let us suppose, as before, that an unknown deposit cell, in addition to the six known deposit cells, occurs in the study area. We will assume that this cell requires the presence of units g8 and g10 as necessary geological characteristics. Four cells out of the six deposit cells in Table 4 have this association. Based on this assumption, the probability that a particular cell of the 169 cells with that association (see Fig. 18), is the unknown deposit cell is $p_1 = (169-4)^{-1} \times (4/6) = 0.40\%$. However, four of the six deposit cells are included in the 84 highest value cells of Fig. 19. This implies that the probability that a randomly chosen cell among the 84 is an unknown deposit cell is $p_2 = (84/4)^{-1} \times (4/6) = 0.83\%$, i.e. twice the value of the previous probability p_1 .

The same control area and five variables were employed in experiments using logistic regression analysis. Contrary to principal component analysis (in which the characteristics of the control area as a whole were the target) logistic regression analysis compares the differences between deposit cells and the remaining cells in the control area. From the regression model, the probability index map shown in Fig. 20 was constructed. The 32 cells with the symbol (/) represent the cells with the highest value; next highest are 75 cells with the symbol (\). These 107 cells

with high values contain three known deposit cells, symbol (o). This shows that the distinction between the deposit cells and the surrounding cells in the control area is very weak. This lack of correlation also became apparent in other statistical tests performed during the analysis.

It can be seen that the patterns of the cells with the highest scores (/) in Figs. 19 and 20, are almost identical. This implies that the regression line and the first principal component axis are closely related to each other. A geological interpretation of this relationship cannot be given at this time and would require further work.

When few occurrences of a given type of mineralization are known, it may be difficult to find characteristics which they have in common and by which deposit cells can be distinguished from cells without occurrences. Without such characteristics, there are severe limitations to this method of evaluation of the potential for unknown resources unless: (1) control areas are established that are far removed geographically from the region being assessed, and (2) the consequent extrapolation is considered not only acceptable but also warranted and unlikely to introduce a serious bias in the results. The probability that a cell with a high value on the probability index map contains one or more undiscovered Cu-Ni deposits, is less than 0.01. Thus the statistical modelling for copper-nickel mineralization, like that for gold occurrences in Archean volcanic rocks (Type 7), has been less successful than that for volcanogenic massive sulphide deposits (Type 1) and for copper mineralization in intermediate-mafic volcanic rocks (Type 16).

SUGGESTIONS FOR FURTHER WORK

The study could be extended to treat additional commodities or deposit types. For example, the region contains a significant number of uranium occurrences, for some of which information is available about the local geological environment. Because of the general geology of the region, significant uranium potential seems likely and therefore investigation of this commodity would be warranted.

Variable g10 (intermediate-mafic intrusive rocks) turned out to be important in the statistical experiments conducted for deposits of Types 1 and 16. However, this variable is very generalized at this stage because it contains a number of different rock types which should be distinguished separately in future work.

Because of the limited resolution afforded by the 500 m distance between picture elements in the east-west and north-south directions, relatively thin formations of felsic volcanic rocks and banded iron formations could not be adequately quantified, despite their metallogenic importance. It will, however, be possible to construct a pattern of curved line segments for these variables by the method used in the present study to quantify contacts between rock types.

The "best" results were obtained for deposits of Type 1. It is interesting to compare these results with those for a well explored area with major producing mines, such as the Abitibi area of Ontario and Quebec. Appendix 3 of Agterberg et al. (1972) is a probability index map for that region, with 38 highest values (>10) for cells measuring 10 km on a side like those used for the present study. Sixteen of those 38 highest values are deposit cells. In total there were 27 deposit cells containing one or more large copper deposits, nearly all of the volcanogenic massive sulphide type. Using the simple method of the present study, the probability that one additional highest value cell is a deposit cell amounts to $(38-16)^{-1} \times (16/27) = 2.69\%$. This is close to $(20-16)^{-1} \times (4/11) = 2.34\%$ obtained for Type 1 in this report. However, in the southern District of Keewatin only 4 of 11 or 36% of known occurrences for Type 1 occur in highest value cells,

whereas in the Abitibi area, 16 of 27 or 59% of large deposits satisfy this criterion. Moreover, the number of deposit cells was larger in the Abitibi study (27 versus 11).

A future direction for the project may be to consider control areas outside of the District of Keewatin, particularly for deposit Types 6 (Cu-Ni) and 7 (Archean-hosted Au) for which relatively poor results have been obtained in this study. These new control areas could be taken from part of the Superior Province or in the Slave Province.

Aeromagnetic data and geochemical information can be used in the course of Phase II of the project. More sophisticated "merged" quantitative appraisals will require a further improvement of the mineral deposit data base and should be spearheaded by qualitative (deposit analogy) appraisals. The construction of an improved and larger geological, geophysical and geochemical data base consisting of digital images for the southern District of Keewatin will stimulate special studies to correlate and integrate different types of geoscience data. A special study of this type dealing with the preferred orientations of Bouguer anomaly contours is described in Appendix 1 of this report.

REFERENCES

- Agterberg, F.P.
1979: Algorithm to estimate the frequency values of rose diagrams for boundaries of map features: Computers and Geosc., vol. 5, no. 2, pp. 215-230.
- Agterberg, F.P., Chung, C.F., Fabbri, A.G., Kelly, A.M., and Springer, J.S.
1972: Geomathematical evaluation of copper and zinc potential of the Abitibi area, Ontario and Quebec: Geol. Surv. Can., Paper 71-41, 55 p.
- Chung, C.F.
1979: A system of interactive graphic programs for multivariate statistical analysis for geological data: Proc. 12th Symp. on Interface of Computer Sciences and Statistics, Univ. of Waterloo, pp. 452-456.
- Davidson, A.
1970a: Precambrian geology, Kaminak Lake map-area, District of Keewatin: Geol. Surv. Can., Paper 69-51, 27 p.
1970b: Eskimo Point and Dawson Inlet map-areas (north halves), District of Keewatin 55E and 55F (north parts): Geol. Surv. Can., Paper 70-27, 21 p.
- Eade, K.E.
1966: Kognak River (west half), District of Keewatin 65G (east half): Geol. Surv. Can., Paper 65-8, 12 p.
1973: Geology of Nueltin Lake and Edehon Lake (west half) map-areas, District of Keewatin: Geol. Surv. Can., Paper 72-21, 29 p.
1974: Geology of Kognak River area, District of Keewatin, Northwest Territories: Geol. Surv. Can., Mem. 377, 66 p.
- Eade, K.E. (cont.)
1978: Notes on metamorphism in Southern District of Keewatin: Geol. Surv. Can., Paper 78-10, p. 191-194.
- Geological Survey of Canada
1980: Preliminary mineral resource appraisal of parts of Yukon and Northwest Territories including proposed northern parks areas: Geol. Surv. Can., Open File 691.
- Gibb, R.A., and Halliday, D.W.
1974: Gravity measurements in southern District of Keewatin and southeastern District of Mackenzie, N.W.T.: EMR Gravity Map Series, Earth Physics Branch, Nos. 124-131.
- Heywood, W.W.
1973: Geology of Tavani map-area, District of Keewatin: Geol. Surv. Can., Paper 72-47, 14 p.
- Kasvand, T., Fabbri, A.G., and Nel, L.D.
Digitization and processing of large regional geological maps: Report, Electrical Engineering Div., National Research Council Canada. (in press)
- LeCheminant, A.N., Blake, D.H., Leatherbarrow, R.W., and deBie, L.
1977: Geological Studies: Thirty Mile Lake and Macquoid Lake map-areas, District of Keewatin: Geol. Surv. Can., Paper 77-1A, p. 205-208.
- Leech, G.B.
1975: Project Appalachia, Geol. Surv. Can., Paper 75-1, pt. C, pp. 121-122 (introduces 8 reports in *ibidem*, pp. 123-173).
- Ridler, R.H.
1971: Relationship of mineralization to stratigraphy in the Archean Rankin Inlet-Ennadai belt, as compared with analogous "greenstone" belts of the Superior Province: Can. Mining J., v. 92, No. 4, p. 50-53.
- Ridler, R.H. and Shilts, W.W.
1974: Exploration for Archean polymetallic sulphide deposits in permafrost terrains: An integrated geological/geochemical technique; Kaminak Lake area, District of Keewatin: Geol. Surv. Can., Paper 73-34, 33 p.
- Stockwell, C.H.
1972: Nueltin Lake granites, Manitoba and District of Keewatin: Geol. Surv. Can., Paper 72-23, p. 33-38.
- Wanless, R.K. and Eade, K.E.
1975: Geochronology of Archean and Proterozoic rocks in the southern District of Keewatin: Can. J. Earth Sci., v. 12, p. 95-114.
- Weber, W., Schledewitz, D.C.P., Lamb, C.F., and Thomas, K.A.
1975: Geology of the Kasmere Lake-Whiskey Jack Lake (north half) area (Kasmere project): Manitoba Mineral Res. Div., Geol. Surv. Branch, Publ. 74-2, 163 p.

APPENDIX 1. STATISTICAL EXPERIMENTS ON THE PREFERRED ORIENTATION OF BOUGUER ANOMALY CONTOURS

Figure 21 shows the digitized contours of the 1:500 000 scale Bouguer anomaly gravity maps for the digital image of 915 x 915 picture elements in the western and central parts of our study area. These contours are for 5 milligal intervals. The original contours were constructed by Gibb and Halliday (1974) for data from gravity stations at intervals of about 12 km. The Bouguer anomaly reflects the specific gravity of rocks at deep levels below the surface. Positive anomalies (gravity highs) reflect the existence of rocks of relatively high density, so may indicate, for example, the existence of thick accumulations of unaltered mafic volcanic rocks or ultramafic rocks. Negative anomalies (gravity lows) may indicate the existence of relatively large volumes of sedimentary rocks or low-density felsic intrusive bodies. The anomalies are evident because Bouguer values are computed by using 2.67 g/cm as the average density of rocks.

In a general way, Bouguer gravity anomaly contours indicate the structural trends of the subsurface rocks. For example, the folded contact between sequences of mafic volcanic rocks and sedimentary rocks presents a density contrast that may be reflected in a Bouguer anomaly at the surface. For this reason, it is of interest to study the preferred orientations of the gravity contours.

Clearly many Bouguer anomalies in Fig. 21 have a northeast-southwest trend whereas others seem to be oriented perpendicular to this direction. We were interested in the relative strengths of the preferred orientations in different parts of the study area. The northeast-southwest trend is particularly prominent in the Snowbird Lake high and, to a lesser extent, the Kazan River high, of Gibb and Halliday (1974).

A simple way to study the rose diagram of the contours in a given subarea is to approximate the contours by successive straight line segments that are sufficiently short, and to plot the histogram of the combined length of all line-segments pointing in directions bounded by class limits (e.g. within 10° or 22½° azimuth zones). When the objective is to determine the preferred orientations, an alternative method consists of first obtaining measurements for narrower class intervals (e.g. 1° or 2°) and then to construct a moving average for wider classes in order to reduce the random fluctuations that generally arise when the classes are very narrow.

A computer program called RODIA (for rose diagram) was developed recently (Agterberg, 1979) that constructs a smoothed histogram for the contact between the two phases ("black" and "white") in a binary image. The input for RODIA is either a relatively small binary image or the so-called geometrical covariance of a larger binary image. This covariance can be computed by means of GIAPP.

Several experiments were performed on the image shown in Fig. 21. First it was changed into the "zebra map" of Fig. 22 which constitutes a binary image. Next a square subarea of 768 x 768 picture elements was outlined on the zebra map with boundaries in the east-west and north-south directions that are at least 5 picture elements removed from the boundaries of the zebra map. The 768 x 768 square was divided into subareas according to two different methods. The first set of subareas is shown in Fig. 23. Area A is roughly triangular and covers the northwestern part of the region; Area B is a SW-NE directed strip across the centre; and Area C covers the southeastern part of the region. A second set of subareas was obtained simply by dividing the 768 x 768 binary image into nine equal-area 256 x 256 binary images for areas labelled 1 to 9 (for locations, see Fig. 26).

Each of the patterns of Fig. 23 was shifted across the pattern of Fig. 22 for distances of 0 to M=5 picture elements in eastern, southern and western directions. The same

procedure was followed for the patterns of Areas 1-9. The number of coinciding black picture elements in the two images was measured for each shift by using GIAPP. The result was a set of 61 covariances which was used as input for RODIA. The choice of input parameters for the program RODIA has been explained in detail by Agterberg (1979). In all cases (Areas A, B, C, and 1-9) it was initially attempted to run the program with M=5 (61 covariances), the exponential model option and smoothing angle A=45°. In a number of instances, these initial input parameters did not give satisfactory results and M=4 was used instead of M=5 (areas B, C and 3) or the linear model instead of the exponential model (areas 1, 4 and 7). These results suggest that, in general, the linear model gives better results when the contours are devoid of relatively sharp curves and more widely spaced. On the other hand, the exponential model is preferable, and simultaneously the number of usable covariances decreases, when the contours show abrupt turns and are close together. In general, to obtain optimum results when RODIA is applied to a binary image a series of experiments should be conducted. Because of the relatively large number (12) of subareas considered in the present study, only one, two, or at most three runs were performed per subarea. The results should be evaluated by comparing histograms for different subareas with one another. Fig. 24 shows the histograms obtained for Areas A, B and C; Fig. 25 is for Areas 1 to 9.

Each histogram should be interpreted as follows. The frequency is plotted vertically. The corresponding direction is plotted for clockwise rotation in the horizontal direction starting from 0 for the west-east direction. Consequently 45 is for the northwest-southeast direction, 90 (in the centre) indicates the north-south direction, 135 is for the southwest-northeast trends and 180 (on the right side) is for the west-east direction. Contours on a map can thus be represented on the semicircle and the value for 180 is equal to that for 0. Fig. 26 shows the relative locations of Areas 1 to 9. Each histogram of Fig. 25 is shown in simplified form in Fig. 26. The frequency values at the local maxima and minima of Fig. 25 were plotted in Fig. 26 at opposite sides of a point at the centre of each area, along lines pointing in the directions of these local maxima and minima.

The patterns of Fig. 24 show that there are two main preferred orientations in Areas A, B and C, with the north-east orientation better developed than the northwest orientation in all three subareas. Both orientations, therefore, seem to be present in the entire study region. Most of the patterns represented in Figs. 25 and 26 confirm the results obtained for Areas A, B and C. However, both of the preferred orientations are less well developed in some subareas than in others.

The strongly preferred orientation of Bouguer contours in Area B (Fig. 25) is comparable to the pronounced northeast trend of the surface rocks, as shown on the geological maps. Similarly in Area 3 (Fig. 26) the northeast trending orientation of gravity contours, including the Snowbird Lake high of the Bouguer anomaly maps, coincides with the trend of exposed rock units, of prominent faults and of pronounced linear features on the aeromagnetic maps.

The northeast trending structure of this whole region is primarily associated with deformation related to the Kenoran orogeny, although in many places it may be overprinted by similar trends related to younger deformation of the Hudsonian orogeny.

The northwest orientation, well developed in Areas 4 and 6 (Fig. 26), is possibly related to younger, high level granite masses, Nueltin Lake granite in the latter area and abundant high level granite plutons younger than the Christopher Island Formation in Area 4. It is therefore suggested that the northwest-southeast orientation represents a younger trend in the crust, associated with granitic plutons that were emplaced after the Hudsonian orogeny.

TABLE 1. Codes for Mineral Deposit and Commodity Types.

<u>Mineral deposit/occurrence Types</u>	<u>No. of occurrences</u>
01 Volcanogenic massive sulphide (VMS)	12
02 U in Archean host rocks	16
03 U in Proterozoic rocks (veins and otherwise structurally controlled)	15
04 U in Proterozoic (sedimentary, Witwatersrand conglomerate type, etc.)	23
05 Base metal veins (polymetallic)	6
06 Cu-Ni in mafic and ultramafic rocks	10
07 Au in Archean volcanic and sedimentary rocks, gneisses, etc.	23
08 Au in Archean iron formation	7
09 Au in Aphebian host rocks	4
10 Unclassified	6
11 Mainly Cu (and subordinate metals) in mafic intrusive rocks	5
13 Mainly Cu in sedimentary and metasedimentary rocks	8
14 Iron Formation	3
16 Mainly Cu in mafic-intermediate volcanic rocks	16
17 Mainly Cu in felsic volcanic rocks	5
18 Disseminated base metals (polymetallic) in volcanic rocks (disseminated equivalent of 1)	3
19 U associated with Archean/Proterozoic unconformities	12
<u>Commodity Types</u>	
01 U-Th	29
02 U-Cu (locally with other metals)	37
03 Au	20
04 Au-Ag, Ag	10
05 Cu (mainly)	29
06 Cu-Ni	10
07 Base metals (and precious metals)	20
08 Base metals (Cu-Zn-Ag) – VMS	10
10 Fe	3
11 Mo, Cu-Mo	2
99 Miscellaneous	4

TABLE 2. Rock units coded for the area classified according to lithology and age.

		Conglomerate sandstone, arkose	Pelite	Carbonate	Greywacke	Iron Formation	Intercalated sediment and volcanics	Felsic volcanic rocks	Undifferentiated volcanic rocks	Mafic volcanic rocks	Alkalic plutonic rocks	Felsic plutonic rocks	Intermediate to mafic plutonic rocks	Mafic plutonic rocks	Ultramafic plutonic rocks	Gneisses
Paleozoic				40												
HELIKIAN	Upper	35		36						38						
	Lower	30					31	37			34	39				
	Undivided											27	28			29
APHEBIAN	Ennadai Lake				26											
	Hurwitz	18	19	20	21			24								25
	Montgomery L.	16														
APHEBIAN/ ARCHEAN												13		14		15
ARCHEAN		1			3	4	5	6	7	8		9	10		11	12

TABLE 3. Summary statistics for statistical experiments performed.

Deposit type	Study area no. of deposit cells	total no. of cells	Type of analysis	Control area no. of deposit cells	total no. of cells	Variables considered	Signif. level for selection	Variables selected for prob. index map	Values for prob. index min. max.	Fig. no.
1 (Volcanogenic massive sulphide deposits)	11	644	Stepwise Regression	11	644	g3,g6,g7,g8,g9, g10,g6xg9,g6xg10, g7xg9,g7xg10, g8xg9,g8xg10	0.4	g7xg10,g6xg10, g7,g10,g8 g6xg9,g8xg10	-0.0447 0.2038	6
	11	644	"	11	356	"	0.4	g7,g6xg10,g10, g6xg9,g8	-0.0784 0.2125	7
	11	644	"	6	183	"	0.4	g7xg10,g7xg9, g7,g6xg10	-0.1134 0.2538	8A
	11	644	"	5	177	"	0.4	g10,g7xg9,g8, g6xg10,g6,g7, g7xg10,g6xg9	-0.1054 0.2599	8B
	11	644	"	9	305	"	0.4	g7xg10,g7,g10, g6xg10,g6xg9, g8xg10,g8	-0.0576 0.2036	9
7 (Au in Archean rocks)	15	1599	"	15	1599	g3,AV,g9,g10,g12, and ten cross products	0.1	AV,g3xg6, g3xg10,g9xg10	-0.0300 0.0650	11
	15	644	"	15	644	g3,g9,g10,g12,and six cross products	0.5	g3,g10,g3xg9, g10xg12,g3xg10, g9xg10	-0.0450 0.0770	12
	15	644	Logistic Regression	7	375	--	-	g3,g10,g3xg9, g10xg12,g3xg10, g9xg10	0.0000 0.1000	13
16 (Cu in mafic to inter- mediate volcanic rocks)	12	644	Stepwise Regression	12	644	g3,g6,g7,g8,g9,g10	0.4	g8,g10,g7	-0.0042 0.0766	14
	12	644	"	10	305	"	0.4	g8,g10,g7	-0.0057 0.0934	15
	12	644	"	12	644	g3,g6,g7,g8,g9, g10,g6xg9,g6xg10, g7xg9,g7xg10, g8xg9,g8xg10	0.4	g8,g7xg10, g7xg9,g7,g6xg9	-0.0454 0.1372	16
	12	644	"	10	305	"	0.4	g8,g7xg10, g8xg9,g6xg9, g10,g7xg9	-0.0246 0.1795	17
6 (Cu-Ni)	6	1599	Principal Components	6	143	--	-	g6,g7,g8,g10, g12	-176.50 226.80	19
	6	1599	Logistic Regression	6	143	--	-	g6,g7,g8,g10, g12	0.0050 0.2630	20

TABLE 4. Copper-Nickel in mafic and ultramafic Archean rocks. Distribution of coded rock units in deposit cells.

Deposit cell No.						Map Unit No.	No. of Cells
1	2	3	4	5	6		
					<u>1</u>	g3	616
			1		1	g6	61
1	1					g7	155
<u>1</u>	<u>1</u>	<u>1</u>	<u>1</u>	<u>1</u>	<u>1</u>	g8	560
		1				g9	642
	1	1	<u>1</u>	<u>1</u>		g10	245
<u>1</u>	1					g12	787
<u>1</u>						g15	622
				1		g18	143
4	4	3	3	3	3	Number of the 9 rock units present in each deposit cell	
2	1	1	1	4	1	Number of occurrences in each deposit cell	

Symbol 1 in the table indicates the presence of the rock units, and this symbol is underlined when the rock unit forms the host for the Cu-Ni occurrences in the cells.

Deposit cells are identified by the numbers 1 to 6 shown in Fig. 18.

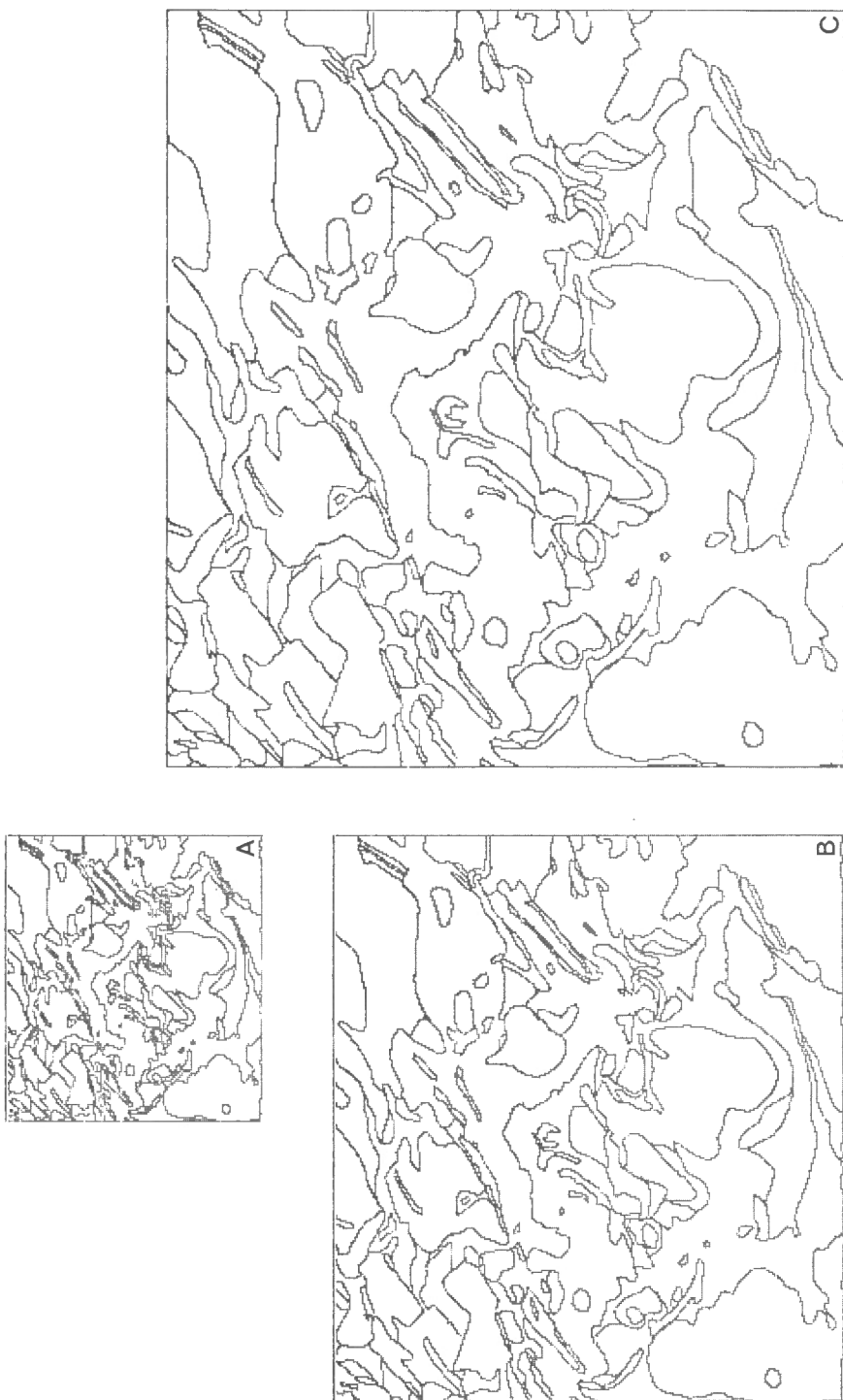


Figure 3. Binary images of square portion of geological map (for location see Fig. 4) obtained at different resolutions from the same vectors: (A) one picture element = 375 m; (B) one picture element = 1000 meters; (C) one picture element = 500 m. These plots were obtained on a Versatec dot matrix printer. The frames are not part of the picture data.

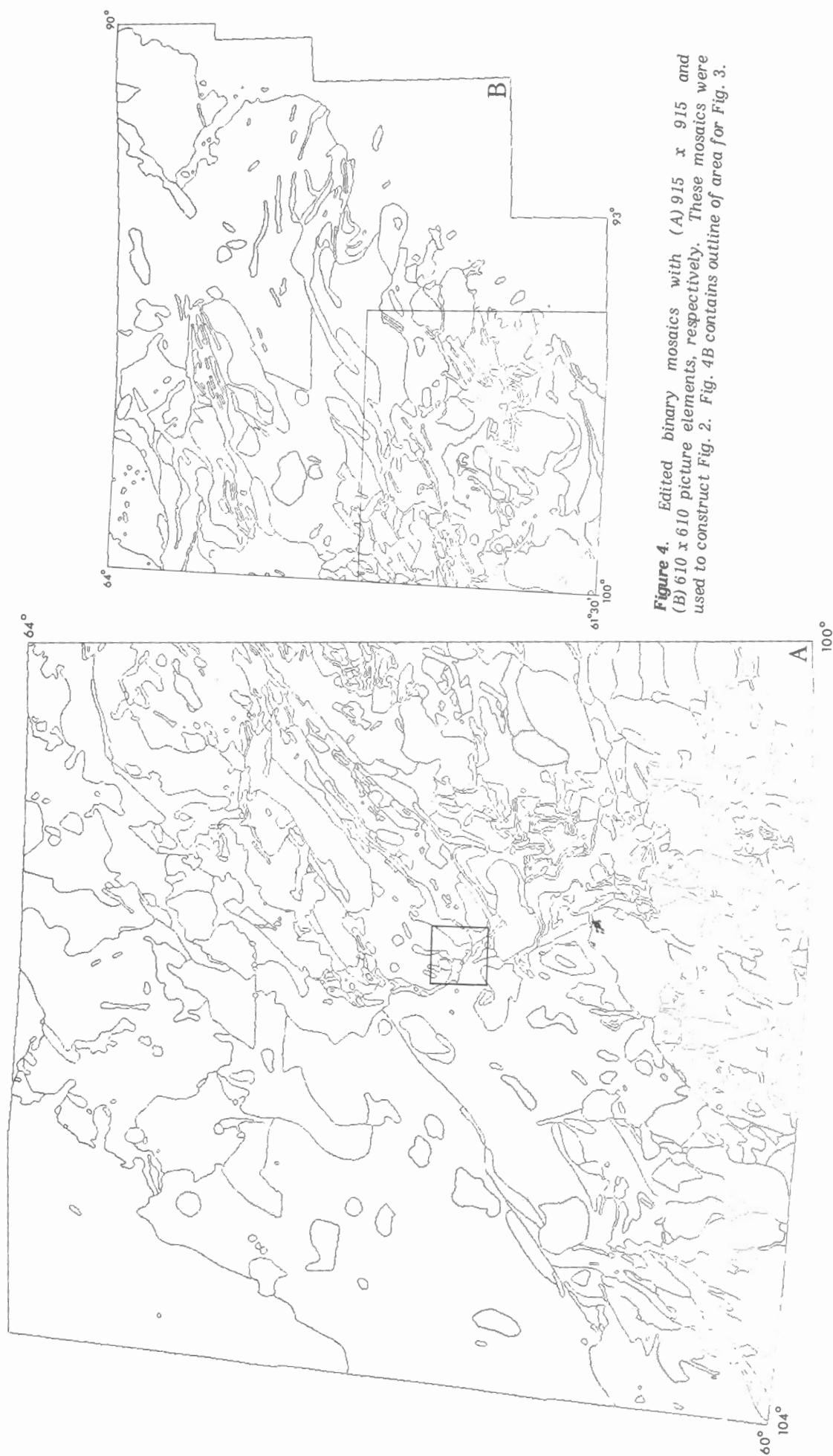


Figure 4. Edited binary mosaics with (A) 915 x 915 and (B) 610 x 610 picture elements, respectively. These mosaics were used to construct Fig. 2. Fig. 4B contains outline of area for Fig. 3.



Figure 5. Line thinning of the binary image of contacts between rock types. A binary mosaic is displayed (A) before thinning and (B) after thinning.

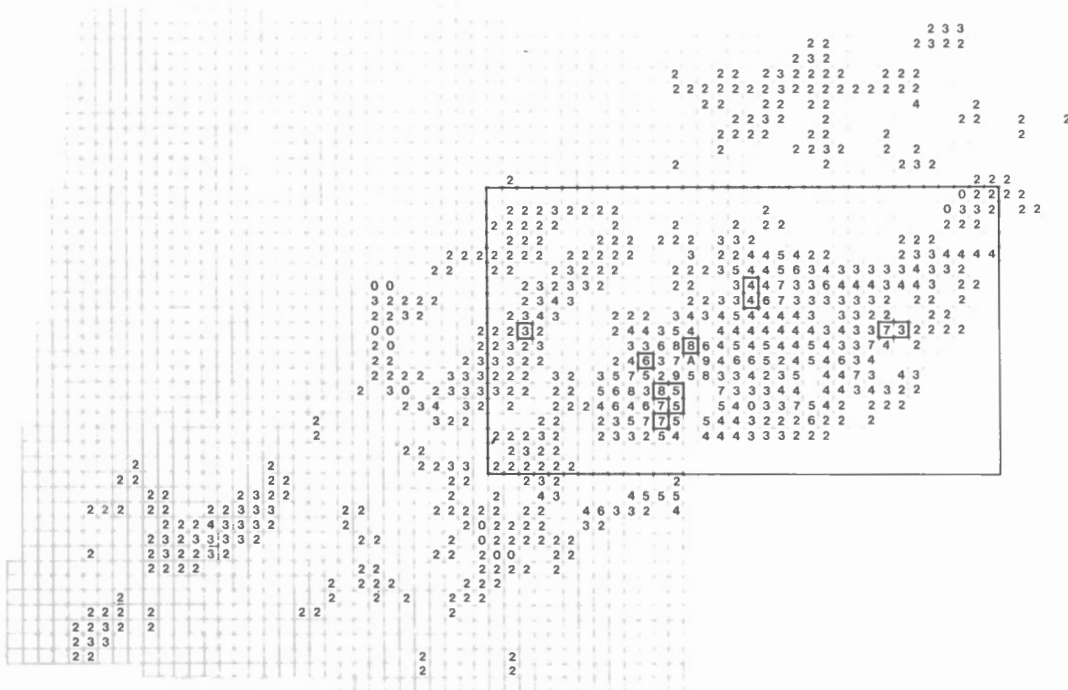


Figure 6. Probability index map for volcanogenic massive sulphide occurrences (Type 1) in cells measuring 10 km on a side. The cells are rated for their relative favourability to contain undiscovered deposits on a linear scale ranging from 0 to 9. The rectangular control area and deposit cells are marked by heavy lines. A indicates largest value in control area and values equal to or greater than this largest value outside a control area. See Table 3 for further details.



Figure 7. Volcanogenic massive sulphide occurrences. Control area of Fig. 6 was divided into two triangular control areas. (A) Probability index map for southeastern portion (based on 6 deposit cells) closely resembles pattern of Fig. 6; (B) Probability index map for northwestern portion (based on 5 deposit cells) shows many high values outside the control area which have not been confirmed by the other experiments.



Figure 8. Volcanogenic massive sulphide occurrences. Experiment of Fig. 6 repeated using different control area.

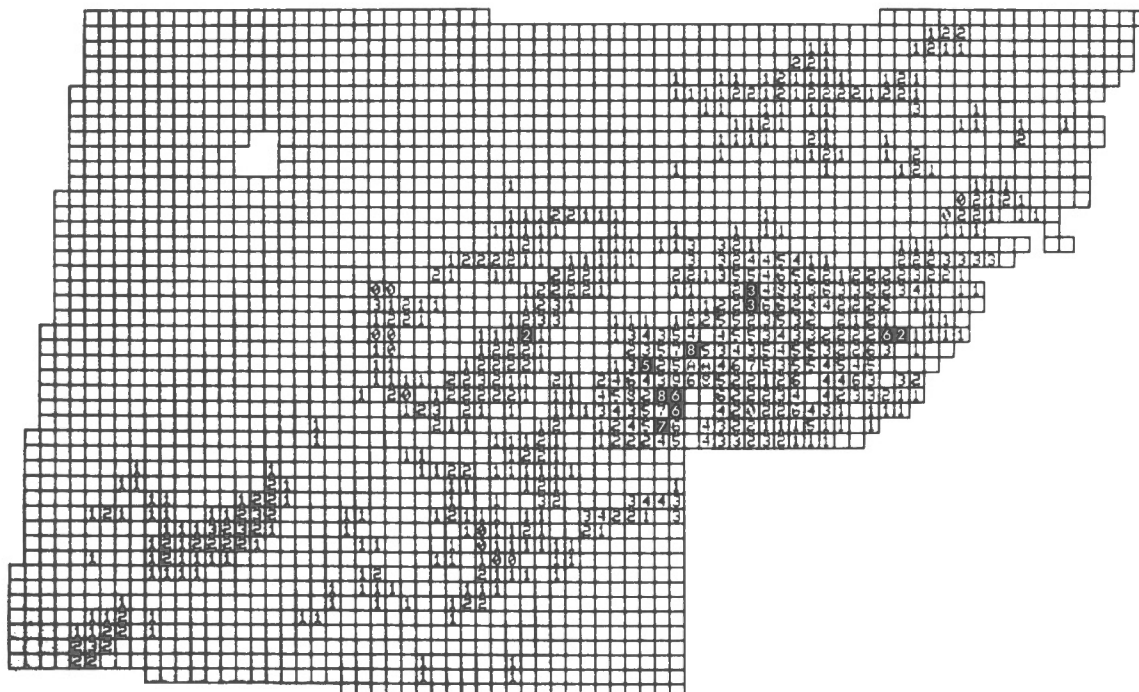


Figure 9. Volcanogenic massive sulphide occurrences. Experiment of Fig. 6 repeated using study area (644 cells) as control area.

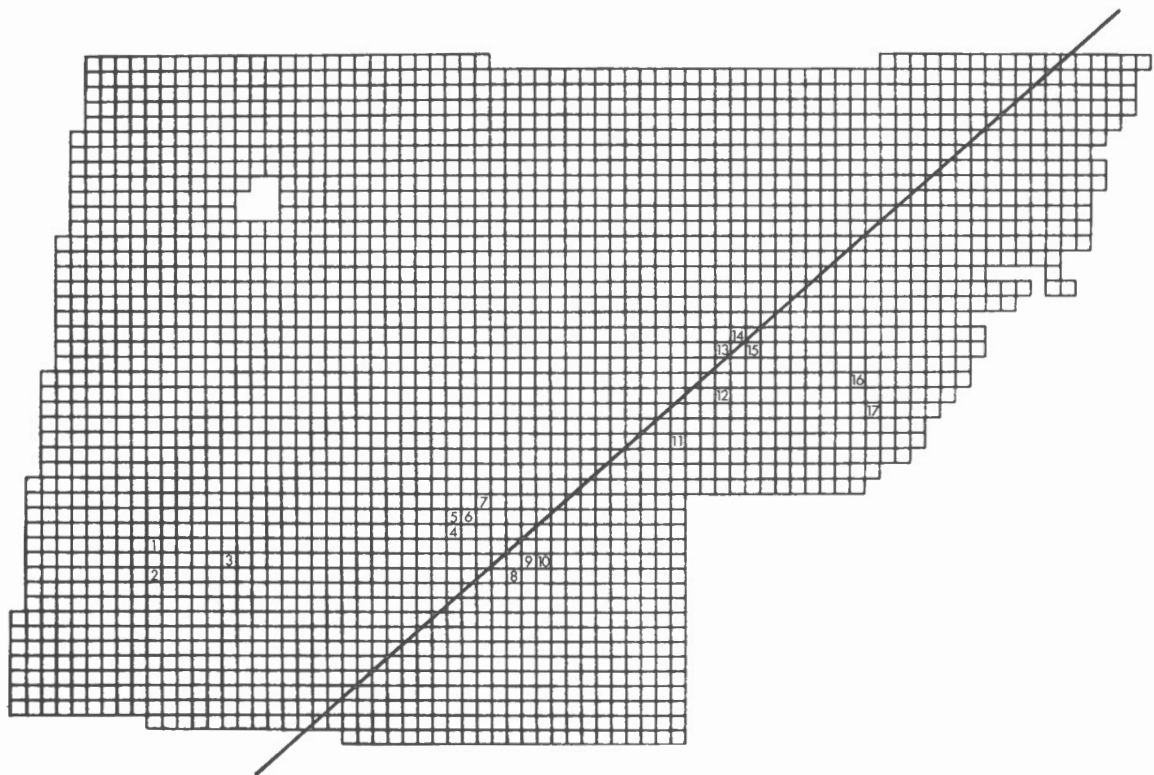


Figure 10. Gold occurrences in Archean volcanic rocks. The 17 deposit cells (numbered 1 to 17) contain 23 occurrences. Diagonal line separates the area into two parts for the experiment resulting in Fig. 13.

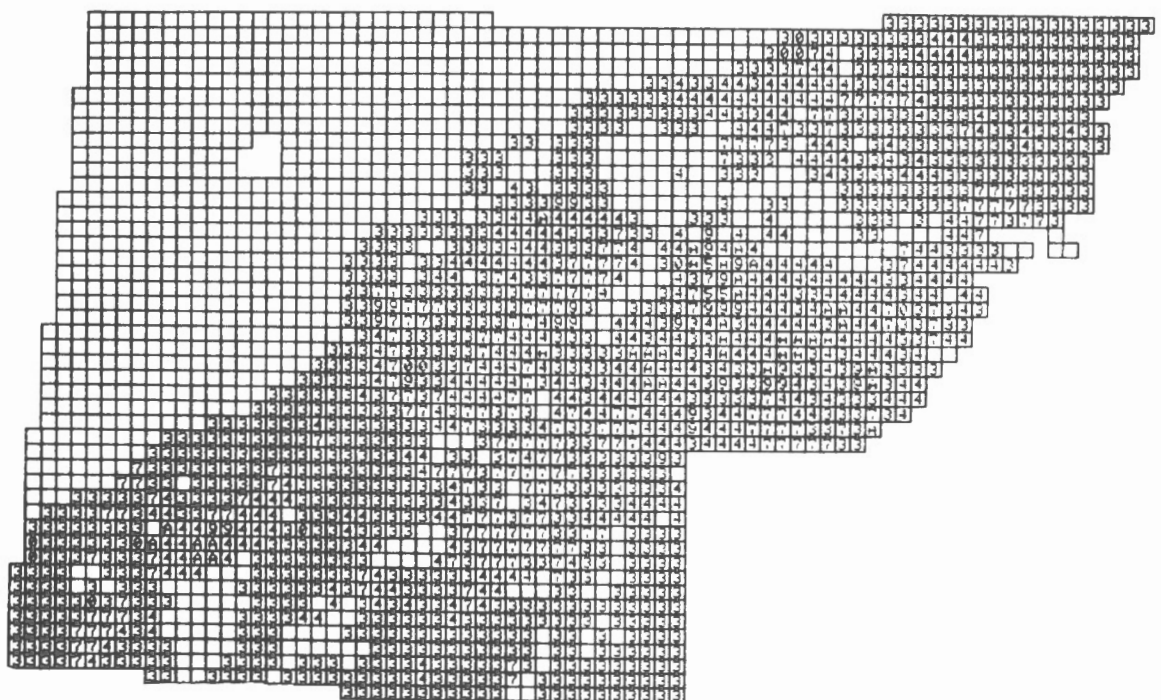


Figure 11. Gold occurrences in Archean volcanic rocks. Study area of 1599 cells containing one or more of 5 variables (g3, g9, g10, g12 or AV) was used as control area. See Table 3 for further details.

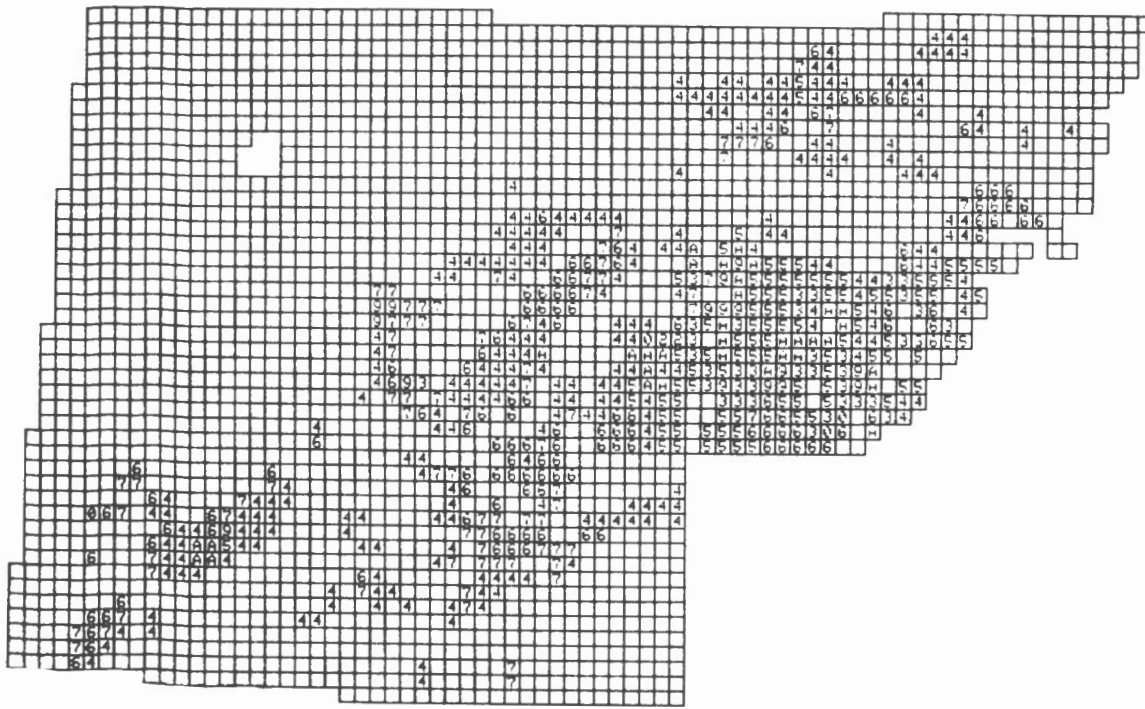


Figure 12. Gold occurrences in Archean volcanic rocks. Study area of 644 cells containing Archean volcanic rocks (AV) was used as control area.

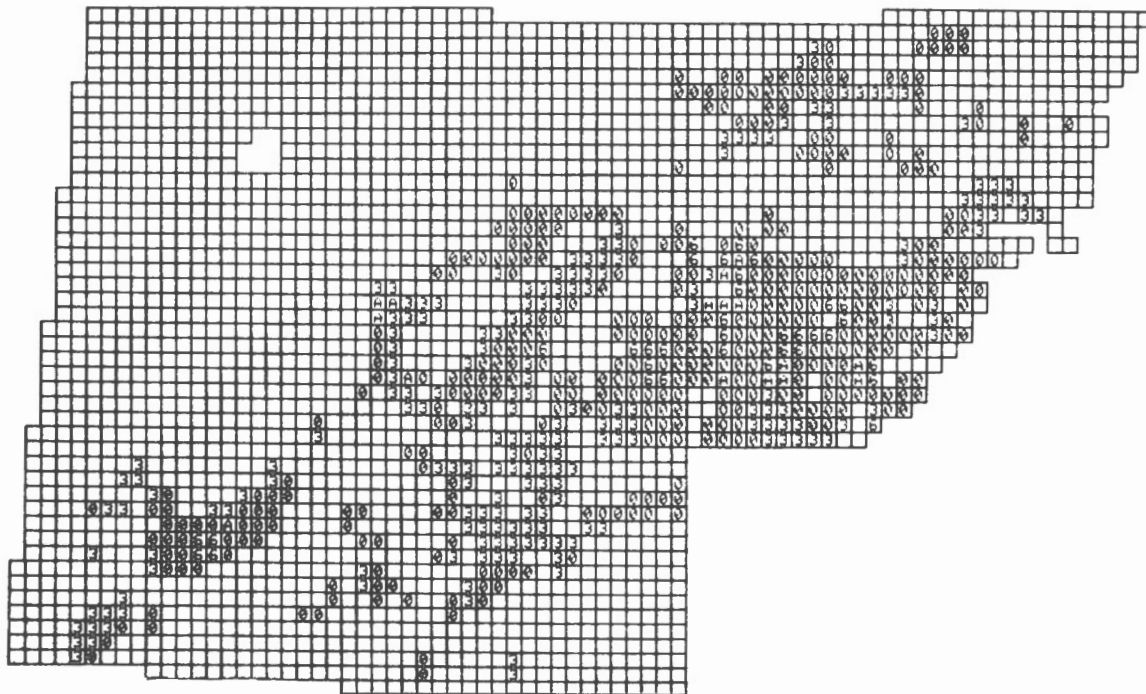


Figure 13. Gold occurrences in Archean volcanic rocks. Portion of area northwest of diagonal line shown in Fig. 10 was used as control area. Variables used are the same as those used for Fig. 12. Logistic regression analysis was applied.

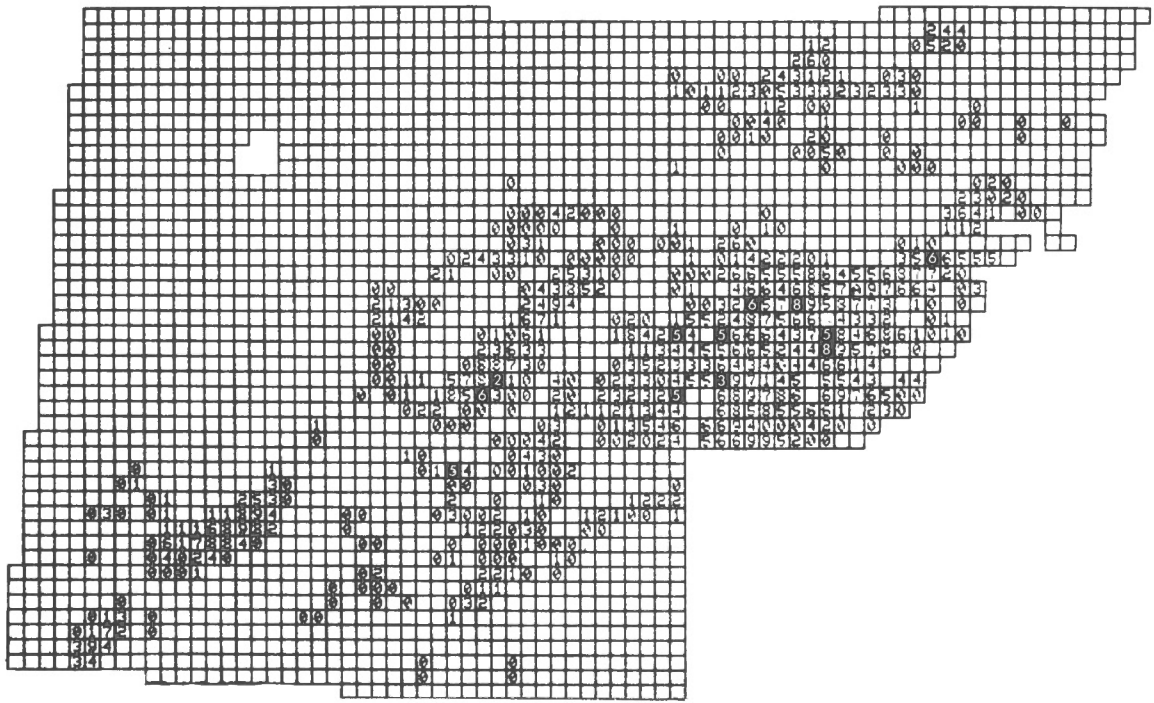


Figure 14. Copper mineralization in intermediate-mafic volcanic rocks. Study area of 644 cells containing Archean volcanic rocks was used as control area. See Table 3 for further details.

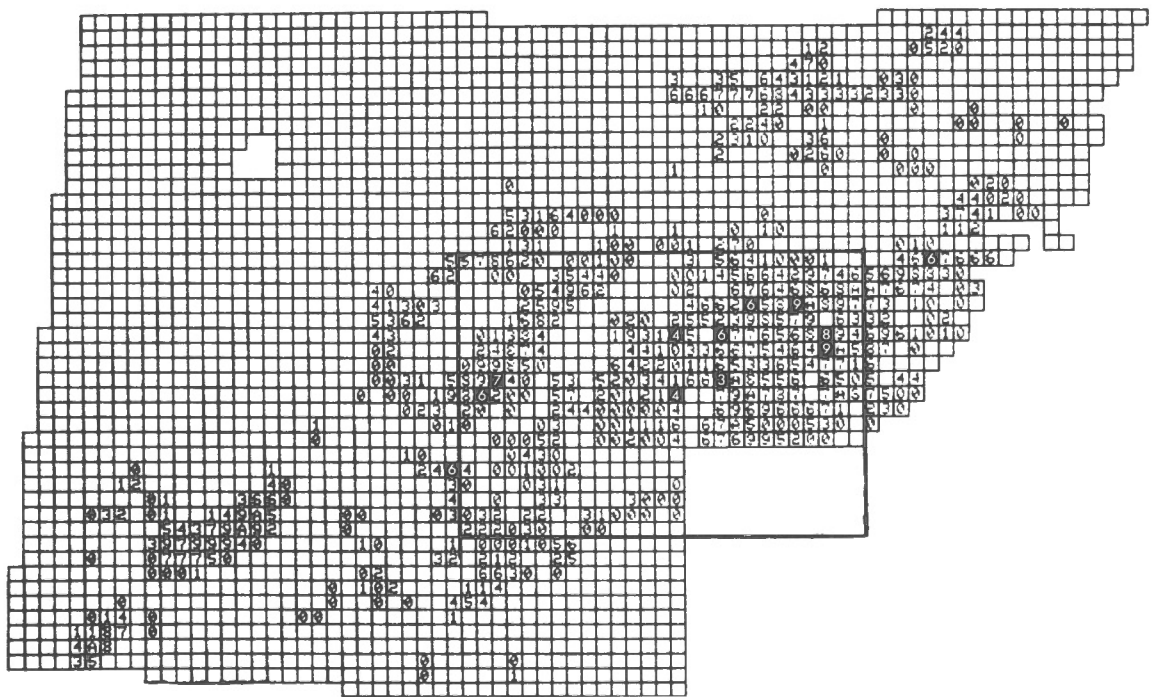
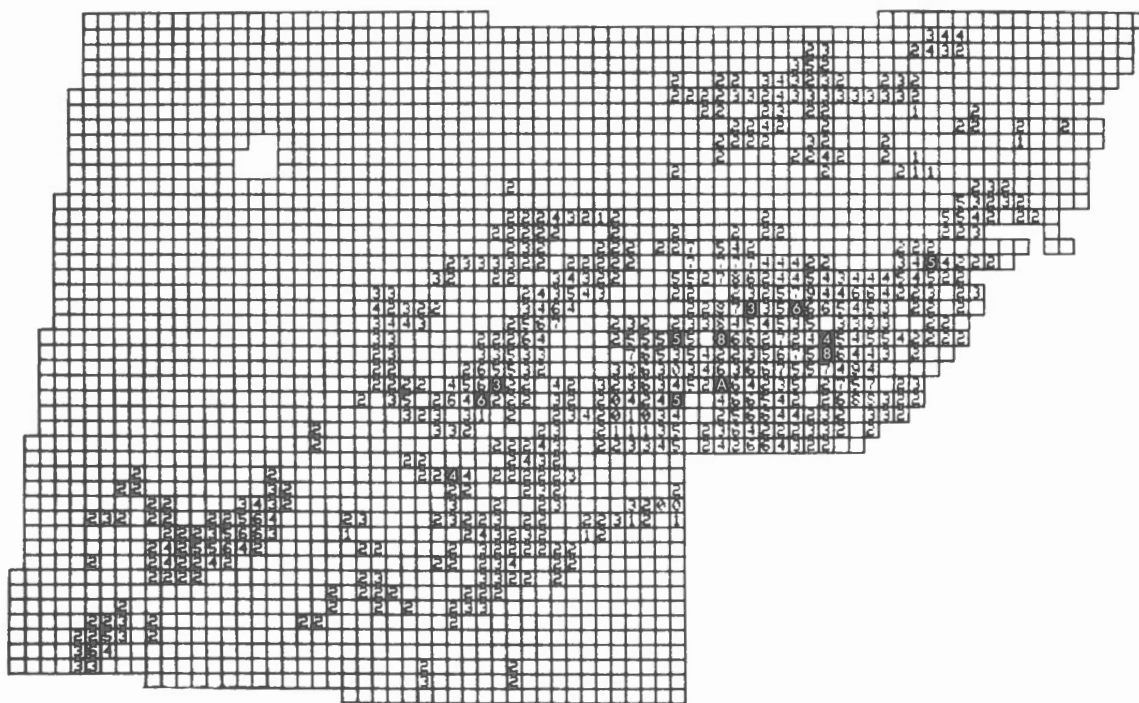


Figure 15. Copper mineralization in intermediate-mafic volcanic rocks. Experiment of Fig. 14 repeated for smaller control area marked by heavy lines.



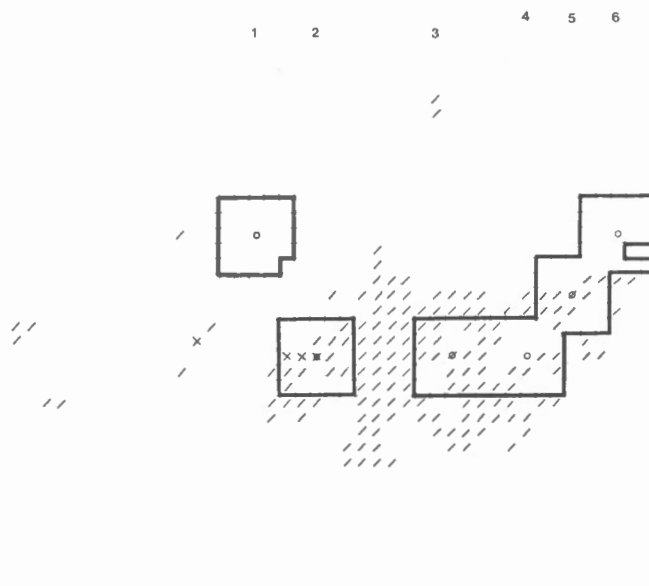


Figure 18. Copper-nickel mineralization in mafic and ultramafic rocks. Six deposit cells (numbers 1 to 6 at top of diagram) are shown as circles. Control area is marked by heavy lines. Also marked are 169 cells containing both Archean mafic volcanic rocks and Archean intermediate-mafic plutonic rocks, and 4 cells with the association (g7, g8, g10 and g12).

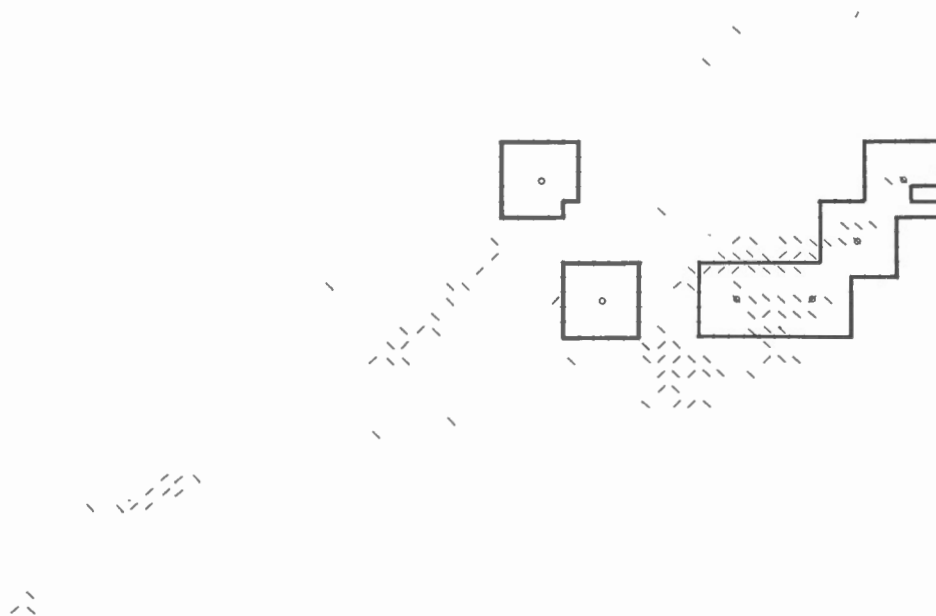


Figure 19. Copper-nickel mineralization in mafic and ultramafic rocks. Principal components analysis was applied to 143 cells of the control area. Highest scores for first principal component are marked in study area of 1599 cells. See text for further explanation.

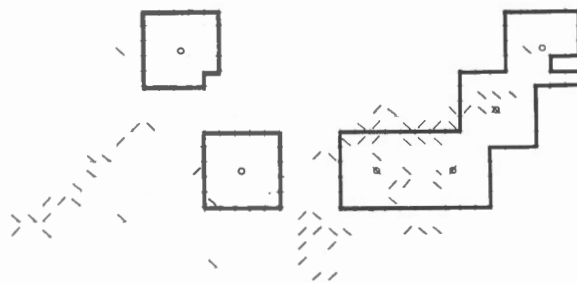


Figure 20. Copper-nickel mineralization in mafic and ultramafic rocks. Experiment of Fig. 19 repeated using logistic regression instead of principal components analysis.

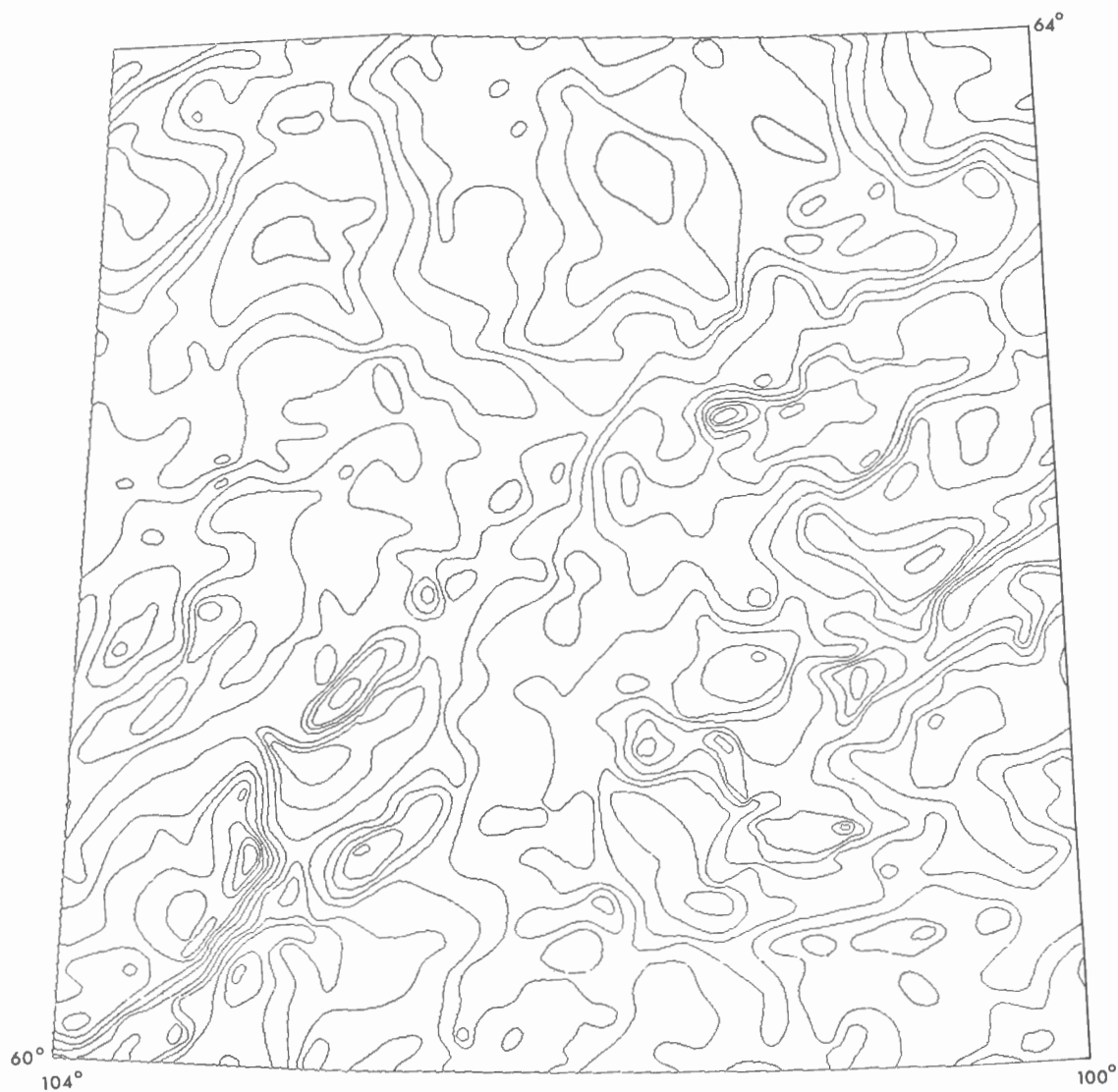


Figure 21. Bouguer anomaly contours for western part of study area, digitized from gravity maps at scale 1:500 000 by Gibb and Halliday (1974).

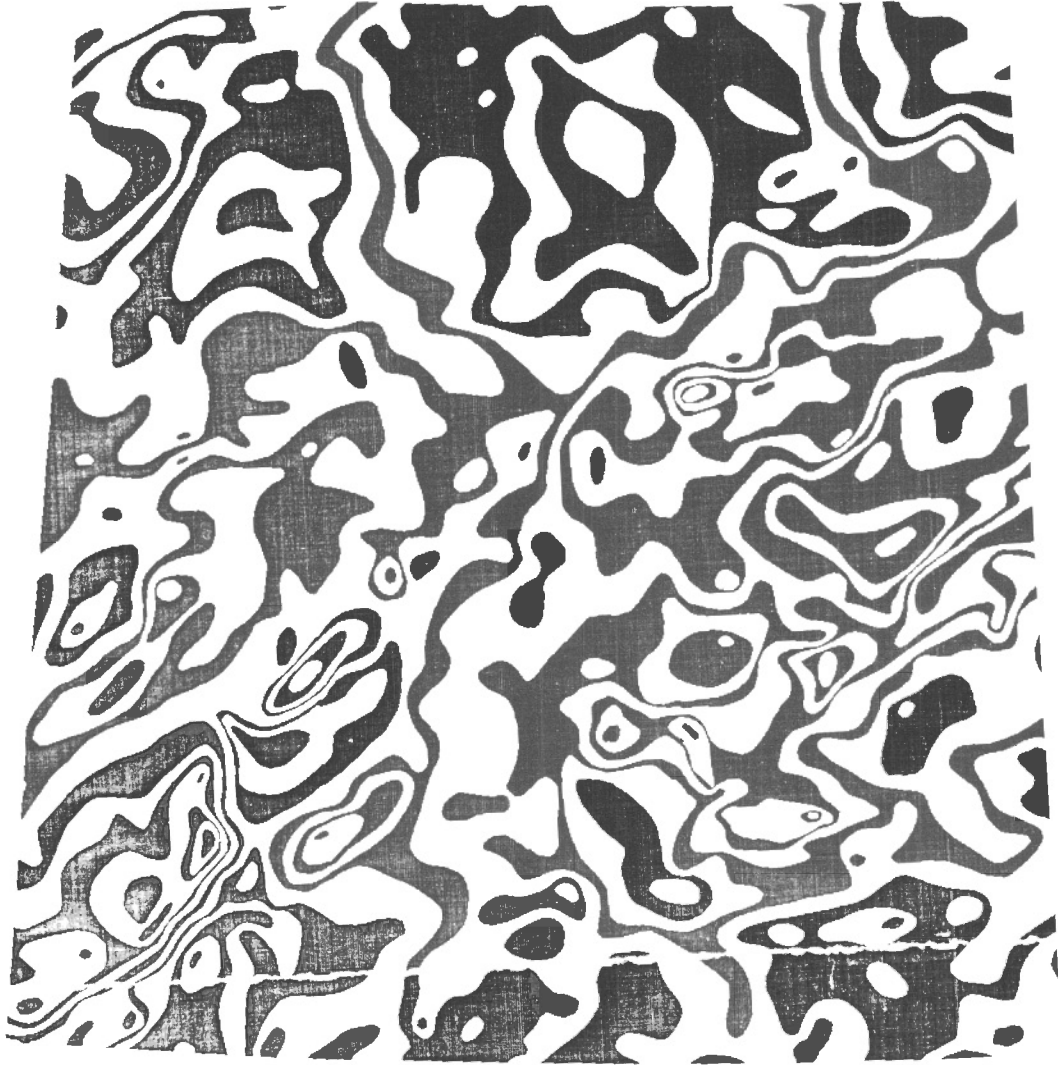


Figure 22. Zebra map for pattern of Fig. 21. The preferred orientations of the boundaries of the black (or white) objects will be studied in subsequent experiments.

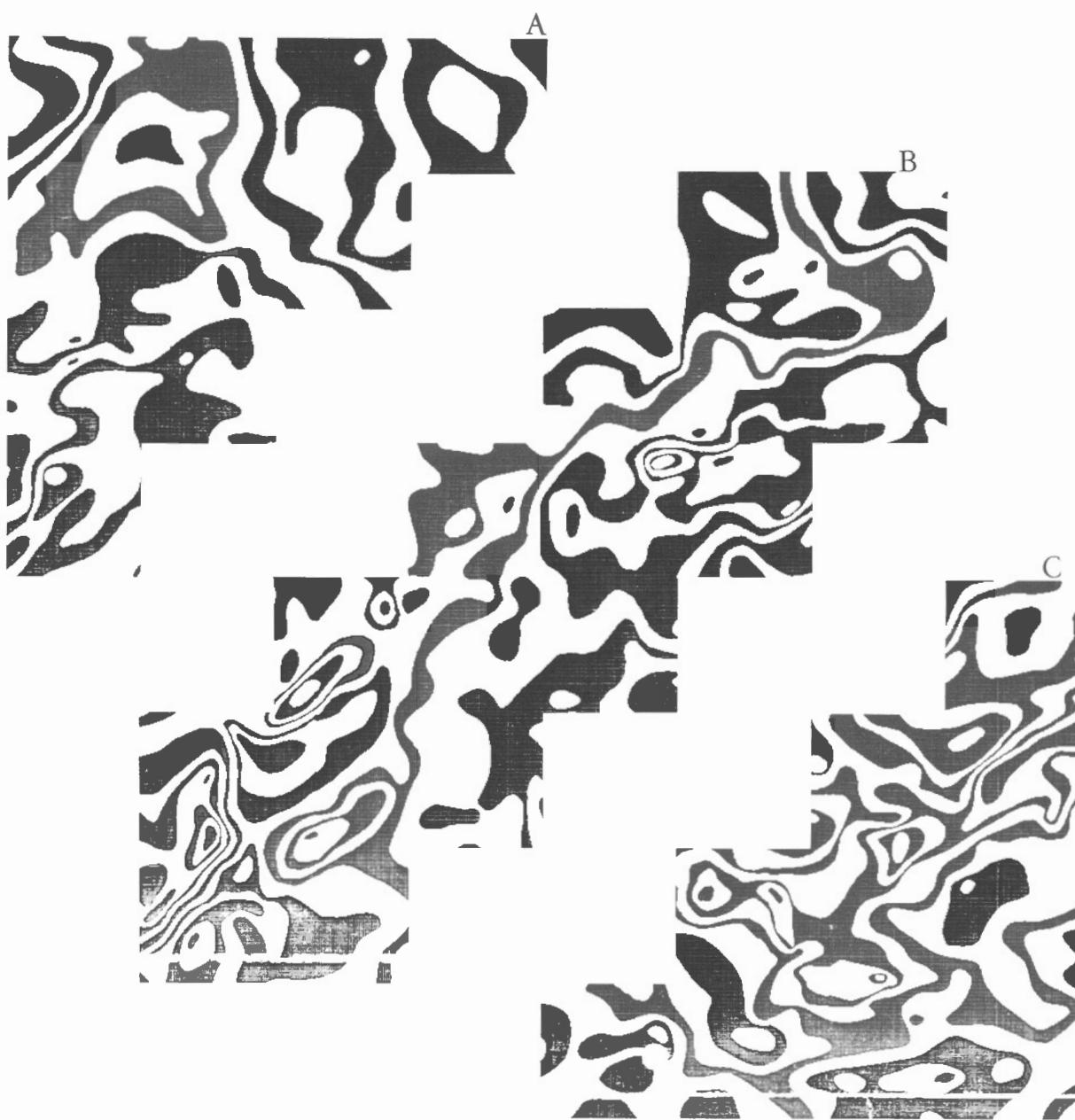


Figure 23. Area of 768 x 768 picture elements covering most of Fig. 22 was subdivided into three subareas (A, B, and C) which were slid across the pattern of Fig. 22 in order to obtain the geometrical covariances.

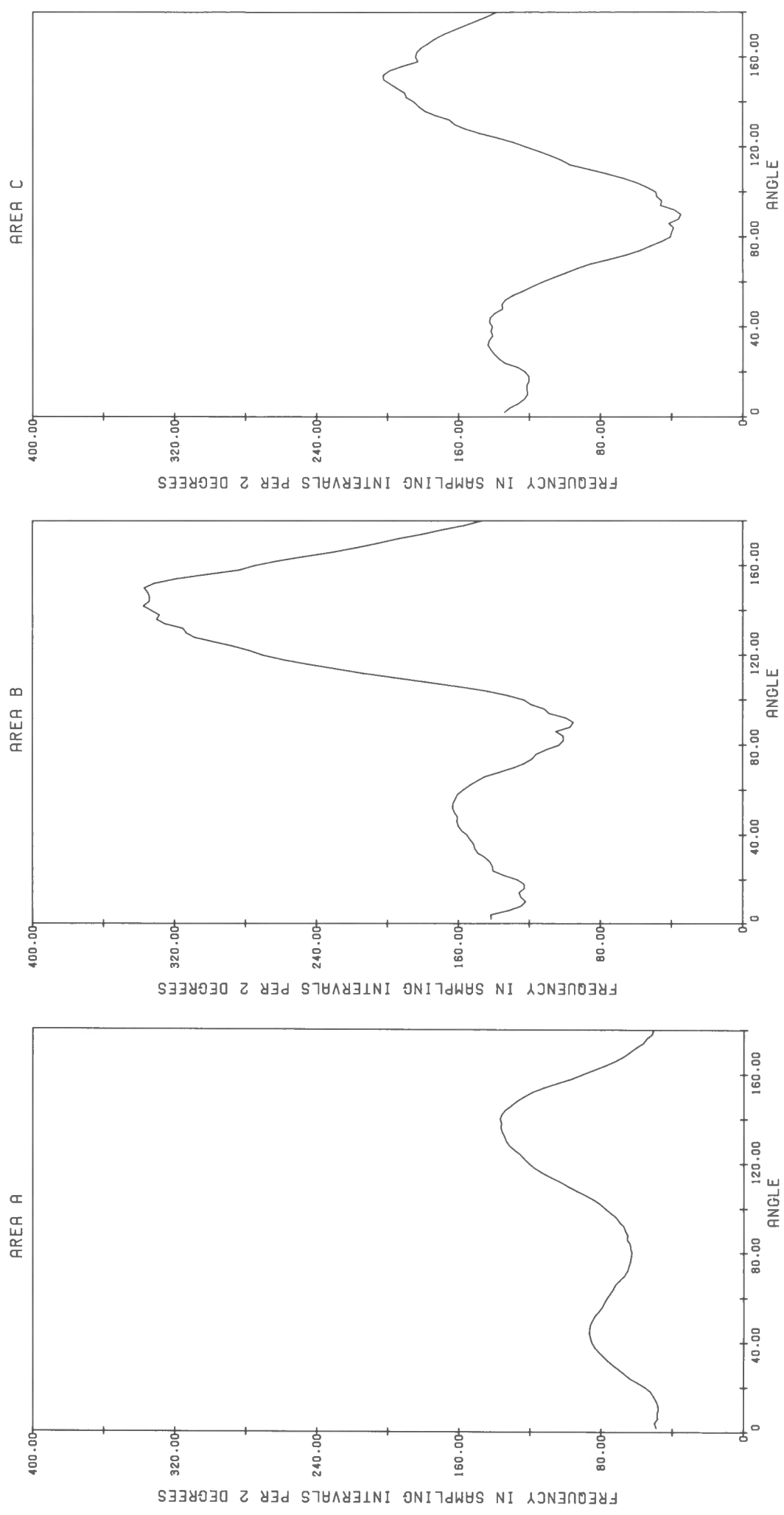


Figure 24. Histograms showing preferred orientations of gravity contours for subareas shown in Fig. 23.
See text for further explanation.

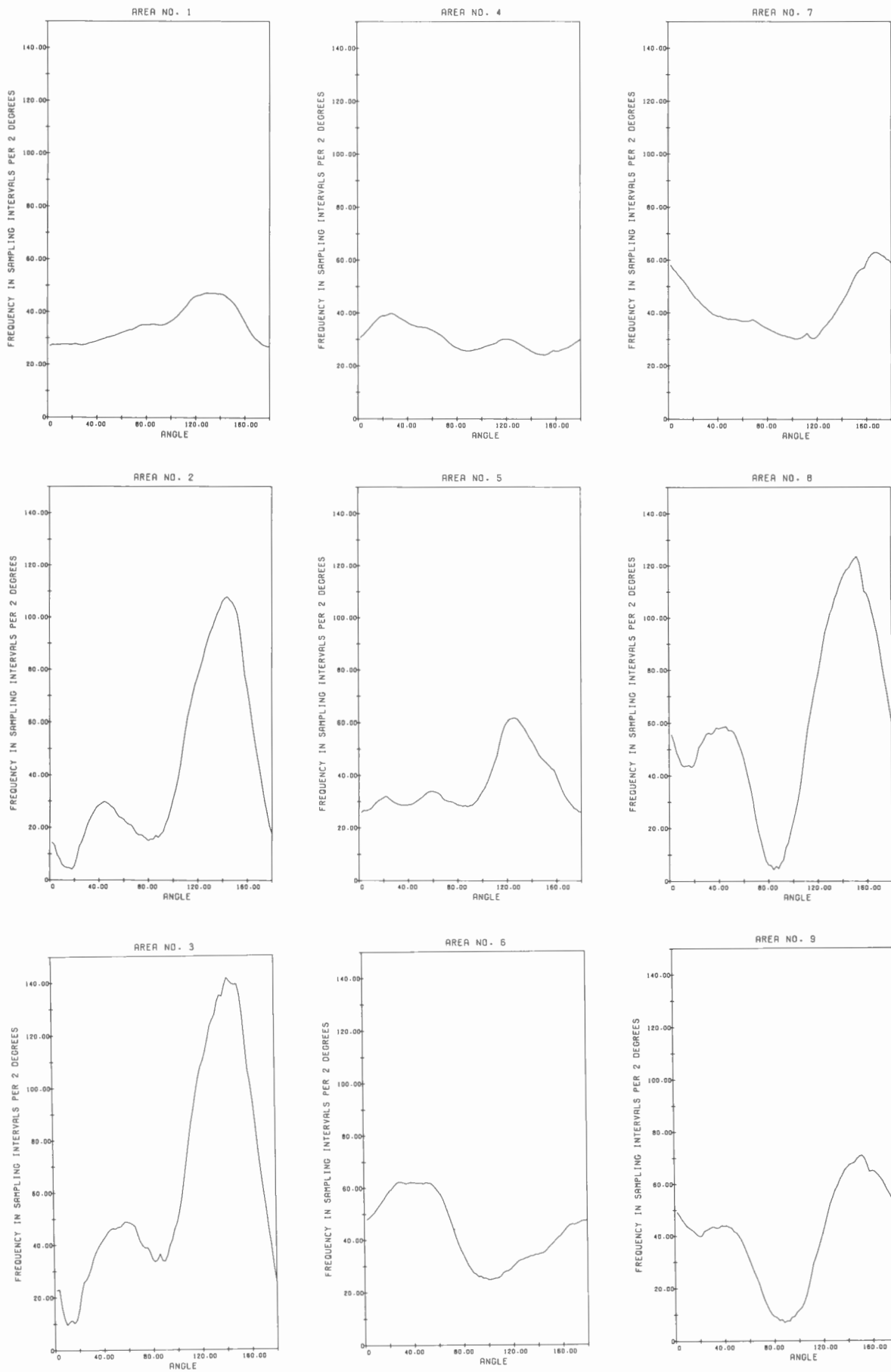


Figure 25. Histograms showing preferred orientations of gravity contours for nine square subareas of which the relative locations are shown in Fig. 26.

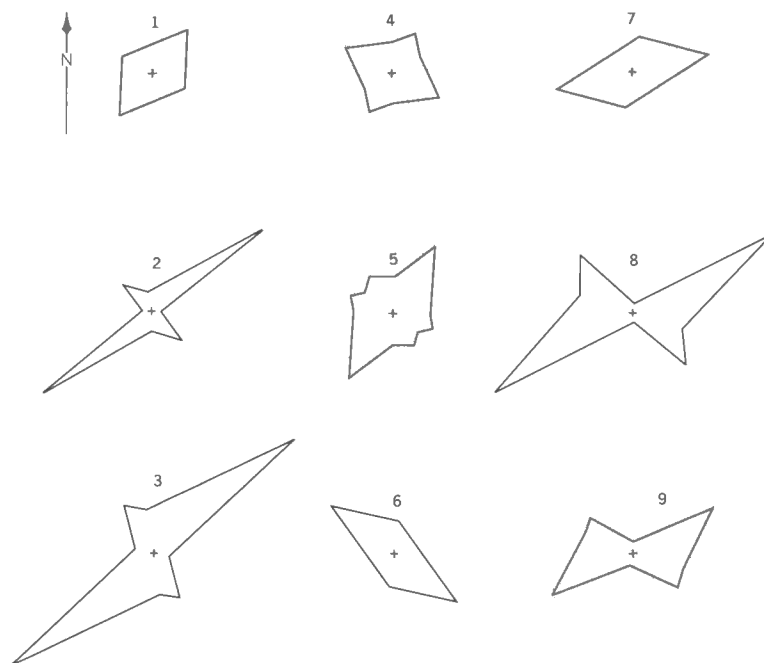


Figure 26. Simplified rose diagrams derived from histograms shown in Fig. 25. Relative maxima and minima were plotted from midpoints of rose diagrams.